Atmos. Meas. Tech. Discuss., doi:10.5194/amt-2016-125, 2016
Manuscript under review for journal Atmos. Meas. Tech.
Published: 6 June 2016

Atmospheric Measurement Techniques
Discussions

Review of the state-of-the-art and future prospects of the ground-based GNSS meteorology in Europe

Guergana Guerova[1], Jonathan Jones[2], Jan Douša[3], Galina Dick[4], Siebren de Haan[5], Eric Pottiaux[6], Olivier Bock[7], Rosa Pacione[8], Gunnar Elgered[9], Henrik Vedel[10], and Michael Bender[11]

[1]Sofia University, Bulgaria
[2]Met Office, United Kingdom
[3]Geodetic Observatory Pecný (GOP), Czech Republic
[4]GeoForschungsZentrum (GFZ), Germany
[5]Koninklijk Nederlands Meteorologisch Instituut (KNMI), Netherlands
[6]Royal Observatory of Belgium (ROB), Belgium
[7]Institut National de l'Information Géographique et Forestière (IGN), France
[8]E-geos s.p.a ASI/CGS, Italy
[9]Chalmers University of Technology, Sweden
[10]Danish Meteorological Institute (DMI), Denmark
[11]Deutscher Wetterdienst (DWD), Germany

Correspondence to: Guergana Guerova, guerova@phys.uni-sofia.bg

Abstract. Global Navigation Satellite Systems (GNSS) have revolutionised positioning, navigation, and timing, becoming a common part of our everyday life. Aside from these well-known civilian and commercial applications, GNSS is now an established atmospheric observing system, which can accurately sense water vapour, the most abundant greenhouse gas, accounting for 60-70 % of atmospheric warming. In Europe, the application of GNSS in meteorology started roughly two decades ago and today it is a well-established research field. This review covers the state-of-the-art in GNSS meteorology in Europe. Discussed are the advances in GNSS processing for derivation of tropospheric products, application of GNSS tropospheric products in operational weather prediction and application of GNSS tropospheric products for climate monitoring. Reviewed are the GNSS processing techniques and tropospheric products. Given is a summary of the use of the products for validation and impact studies with operational Numerical Weather Prediction (NWP) models as well as very short weather prediction (nowcasting) case studies. Climate research with GNSS is an emerging field of research, the studies so far have been limited to comparison with the climate models and derivation of trends.

More than 15 years of GNSS meteorology in Europe has already achieved outstanding cooperation between the atmospheric and geodetic communities. It is now feasible to develop next-generation GNSS tropospheric products and applications that can enhance the quality of weather forecasts and climate monitoring. This work is carried out within COST Action ES1206 "Advanced Global Navigation Satellite Systems tropospheric products for monitoring Severe Weather Events and Climate" (GNSS4SWEC, http://gnss4swec.knmi.nl).

1 Introduction

Atmospheric water vapour has a complex life cycle in the troposphere, including vertical and horizontal transports, mixing, condensation, precipitation, and evaporation. Due to its high temporal variations (more than 50 % within a few hours, Johansson et al. (1998)) and its complex distribution linked to its relationship with atmospheric dynamics and the role of phase changes, the understanding of tropospheric water vapour is of essential importance to climate science and Numerical Weather Prediction (NWP). However, whilst being a critical atmospheric observation parameter, it is also very demanding to observe. Since the 1950s, the standard technique for measuring atmospheric water vapour has been the radiosonde. Whilst radiosondes do provide invaluable atmospheric observations, they do have some inherent limitations, primarily limited temporal and spatial resolution (soundings are typically performed once or twice a day and the spatial coverage of the network in Europe is 250 km or greater). Tralli and Lichten (1990) first proposed to use the Global Positioning System (GPS) for atmospheric sounding. As GPS signals travel through the atmosphere their propagation is affected by atmospheric constituents and in particular water vapour. The technique was first called GPS meteorology and later renamed to Global Navigation Satellite System (GNSS) meteorology. GNSS refers to any satellite constellation with global coverage used for positioning, navigation, and timing. Currently two constellations are fully operational: GPS (USA, NAVSTAR) and GLONASS (Russia). Two other systems are currently under development: Galileo (ESA/EC, with 12 satellites in orbit out of an operational constellation of 30 satellites) and BeiDou (China, with 17 satellites in orbit out of an operational constellation of 35). In this paper we will use the name GPS meteorology when it deals with the standalone GPS and the name GNSS meteorology when it concerns either more than this system or in more general context.

The establishment of GPS meteorology, as an operational atmospheric sounding technique in Europe, was a focus of a number of major European projects (Figure 1). Collaborative activities aiming at the exploitation of GPS observations for monitoring atmospheric water vapour started with the EC 4th Framework Program (FP) projects WAVEFRONT (GPS WAter Vapour Experiment For Regional Operational Network Trials) and MAGIC (Meteorological Applications of GPS Integrated Column Water Vapour Measurements in the western Mediterranean). MAGIC combined the efforts of GPS network operators in France, Italy and Spain to build a GPS demonstration network for weather forecasting in the western Mediterranean area (Haase et al., 2001). In the follow-up EC COST Action 716 (COST-716), 15 European countries participated with the overall aim to provide a European demonstration campaign for GPS meteorology. Operational provision of ground-based GPS Zenith Total Delay (ZTD) products started in 2001 (Elgered et al., 2005). In 2003, MAGIC and COST-716 were followed by the EC 5th FP scientific project TOUGH (Targeting Optimal Use of GPS Humidity Measurements in Meteorology), and in April 2005, the EUMETNET EIG GPS Water Vapour Programme (E-GVAP, http://egvap.dmi.dk) was established to transform GPS meteorology from an R&D activity to a full operational service across Europe. Currently, 18 National Meteorological and Hydrological Services (NMHS) collaborate in E-GVAP with 17 GPS analysis centres (ACs), which collect and process GPS data from over 1800 European ground-based stations (Figure 2).

The present state-of-the-art of GNSS Meteorology would have been impossible without the products provided by the Global Geodetic Observing System (GGOS, http://www.ggos.org). GGOS products are provided by the services of the International

Atmos. Meas. Tech. Discuss., doi:10.5194/amt-2016-125, 2016
Manuscript under review for journal Atmos. Meas. Tech.
Published: 6 June 2016

Association of Geodesy (IAG, http://www.iag-aig.org). One of them is the International GNSS Service (IGS, http://www.igs.org). At present, IGS provides among other wide range of satellite (orbit and clocks) and tropospheric products.

The aim of this paper is to assess the current state-of-the-art of GNSS meteorology in Europe. In Section 2 the development of GNSS tropospheric products processing techniques are reviewed. Section 3 summarises the use of GNSS tropospheric products for operational weather prediction applications like NWP, nowcasting, and monitoring severe weather. Section 4 presents the application of GNSS tropospheric products in climate monitoring. The outlook and future work are given in Section 5.

2 GNSS tropospheric processing

2.1 GNSS observations and the atmosphere

GNSS signals are delayed and bent when propagating through the atmosphere. The upper part of the atmosphere is a dispersive medium which influence can be more or less eliminated by combining observations at two GNSS L-band frequencies in the range from 1.16 GHz to 1.61 GHz. The effect of the lower neutral part of the atmosphere cannot however be eliminated in a similar way because this is a non-dispersive medium. The major effect of the neutral atmosphere occurs in the troposphere. In the following we refer to this effect as tropospheric delays. In accurate GNSS applications, and specifically for our application, the tropospheric delay at each station is estimated, together with other parameters, in the GNSS data analysis.

A common model for the total slant tropospheric delay from the GNSS satellite to the receiver on the surface of the Earth is, see e.g. Teke et al. (2013)

$$\Delta\rho_{rec}^{sat}(e,A) = mf_h(e)\, ZHD \,+\, mf_w(e)\, ZWD \,+\, mf_g(e)\, [G_N\, \cos(A) \,+\, G_E\, sin(A)] \tag{1}$$

where e and A are the elevation and the azimuth angle towards a specific satellite, ZHD and ZWD are the so-called zenith hydrostatic and the zenith wet delays expressed in units of metres, mf_h, mf_w, mf_g are the hydrostatic, wet, and gradient mapping functions, and G_N and G_E are the components of linear horizontal gradients. The first two terms on the right hand side represents a model assuming tropospheric symmetry while the last term may be added in order to estimate a first-order asymmetry in terms of a linear horizontal gradient.

The tropospheric Zenith Total Delay (ZTD) characterizes the effect of the troposphere which delays GNSS signal coming from the zenith. The mean delay is typically about 2.4 m from a site at the sea level. The ZTD is the sum of the ZHD and the ZWD or, alternatively, a sum of an a priori and an estimated tropospheric delay correction. A separation of hydrostatic and non-hydrostatic components was proposed by Davis et al. (1985). The latter is often simply referred to as the ZWD although it represents a non-hydrostatic component complementary to the hydrostatic one. The elevation angle dependencies of ZHD and ZWD are modelled by individual mapping functions with coefficients calculated using climatology, meteorologic data or NWP output.

The ZHD and the ZWD definitions originates from the integrals describing the delay and bending of a signal propagating through the atmosphere with a varying refractivity defined by meteorological parameters. A model for the ZHD was developed by Henriksen et al. (1972)

$$ZHD = 10^{-6} k_1 \frac{R_d}{g_{\varphi,H}} p, \tag{2}$$

where

$$g_{\varphi,H} = 9.784 \,.\, (1 - 0.00266 \cos(2\varphi) - 0.00000028H) \tag{3}$$

where k_1 is a refractivity constant, in KPa^{-1}, R_d is the specific gas constant of dry air (287.058 $Jkg^{-1}K^{-1}$), $g_{\varphi,H}$ is the gravitational acceleration in m/s^2 at the latitude φ and at the station height H, in m, above the geoid, p is the atmospheric pressure, in Pa, at the height H in m.

Since ZWD is a mainly a function of partial water vapour pressure e and the temperature T, it can be calculated with a numerical integration through a full profile of these meteorological parameters together with the two refractivity constants k_2' $[K/hPa]$ and k_3 $[K^2/hPa]$

$$ZWD = 10^{-6} \int_H^{\infty} ({k_2}' \frac{e}{T} + k_3 \frac{e}{T^2}) dh. \tag{4}$$

The above description summarizes the relations between tropospheric parameters used in the GNSS data analysis and the meteorological parameters of interest. A synergy between GNSS and meteorological observations thus offer broad range of applications. Firstly, the capability of estimating tropospheric parameters from GNSS with a high spatial and temporal resolution, a low latency, is of high interest for meteorology. Secondly, since the long term GNSS observations are available globally monitoring of trends in the atmospheric water vapour is also feasable. Thirdly, meteorological or climatologic data are useful when trying to optimize the models used in the GNSS data processing. Fourthly, meteorological or climatologic data can be useful to support high-rate real-time kinematic applications in order to reduce tropospheric errors or, more generally, to avoid high correlations between estimated height coordinates.

Within GNSS tropospheric processing, it is common to distinguish products according to their availability (Table 1) : 1) Final Products (Final) based on daily observations and final precise post-processed products, 2) Near Real-Time products (NRT) based on hourly observations and ultra-rapid precise products, 3) Real-Time products (RT) based on real-time observations and real-time precise products. The Final Products (column 2 in Table 1) have the best possible precision and accuracy, but are available with a delay of between 1 day and 2 weeks after time of observation. Due to their high quality, Final Products are used as reference. The NRT and RT (columns 3 and 4 in Table 1) product accuracy is compromised due to the latency requirements implied by the application. For example, in order to be used in NWP models, the NRT products which are updated hourly have a requested latency of 90 min after time of observation. The RT products have a typical latency of 5-10 min after time of observation and are updated sub-hourly.

The potential of GPS observations for troposphere monitoring was suggested by Tralli and Lichten (1990) and Bevis et al. (1992), but it only concerned Final Products. The development of NRT GPS data processing suitable for operational weather prediction was, however, not possible until 1999 mainly due to 1) the lack of a hourly data flow from the permanent GPS stations and 2) the limited quality of predicted precise satellite orbits and clocks. First operational NRT tropospheric products (Zenith Total Delay, ZTD) for Europe were demonstrated in the early 2000s (Gendt et al., 2001; Dick et al., 2001; Douša, 2001a, b) during the COST-716 benchmark campaign. After this successful benchmark campaign, a demonstration campaign was initiated in 2001 (van der Marel et al., 2004). The demonstration campaign continued without interruption during the TOUGH and E-GVAP I, II, III and IV Projects (see Figure 1). The main purpose of the E-GVAP project is to collect and distribute NRT (within 90 min) GNSS derived ZTDs for usage in operational weather forecasting, to monitor data quality and attempt to expand the GNSS meteorological network in a collaboration between meteorology and geodesy.

2.2 Advanced GNSS processing techniques for NRT and RT products

The current state-of-the-art in GNSS data processing for operational meteorology provides hourly updated NRT ZTD estimates, using mainly data from only the GPS satellite constellation. The majority of the Analysis Centres (ACs) utilize a Precise Network Positioning (PNP) solution eliminating GNSS receiver and satellite clock errors in double-difference observations. Two GNSS ACs provide an alternative approach based on the Precise Point Positioning (PPP) technique (Zumberge et al., 1997), which exploits original data without differencing. The main reason for applying the network approach was the lack of ultra-fast precise satellite clock products required for PPP (see Table 2). The ACs GFZ (German Research Centre for Geosciences, Gendt et al. (2004)) and NGAA (GNSS AC collaboration between Chalmers Technical University and Swedish Meteorological and Hydrological Institute) developed their own techniques for providing global products in support of PPP. Their processing thus resulted in a two-step approach: 1) a common global NRT solution for determining consistent satellite clock and orbit products, and 2) an autonomous, distributed PPP ZTD processing for each station individually.

Significant improvements in GNSS data processing (including models and products) as well as enhanced GNSS infrastructure lead to new challenges. The real-time data and product flows have been developed and standardized, and many GNSS stations from around the world now provide real-time data streams, which are used for generating real-time precise products such as precise satellite clock corrections. In 2013, the International GNSS Service (IGS, Dow et al. (2009)) launched its Real-Time Service (Caissy et al., 2012) providing precise satellite orbit and clock corrections in support of ultra-fast or real-time PPP processing (Douša and Vaclavovic, 2014; Li et al., 2014a; Yuan et al., 2014). Tropospheric products of real-time PPP processing are of high interest for NWP models and for nowcasting of severe weather events.

Along with the standard estimation of ZTD, several ACs monitor the tropospheric asymmetry by estimating tropospheric horizontal gradients. In addition, retrieval of the Slant Tropospheric Delay (STD), i.e. the total tropospheric delay in the direction from the receiver to a visible satellite, can provide additional information about the atmospheric structure (see Figure 3). One important application of STDs are their use for tomographic reconstruction of the 3D water vapour fields (see Section 3.3). However, tomographic reconstruction depends to a large extent on the quality of the STD estimates. The PPP processing method for producing STDs is preferred due to its efficiency, namely 1) easy support of additional estimated parameters in the distributed processing system, and 2) the capability of directly providing undifferenced slant delays from PPP. However, this strategy requires precise satellite orbits and clocks products, and the most accurate models.

The processing of individual STDs is currently an active field of research and different approaches are considered. One strategy is to rely on the combination of the well-established production of ZTDs and horizontal gradients to map this information to the direction of the GNSS signal path. Several variations are used: 1) mapping of the zenith delay on the slant axis (Notarpietro et al., 2011), 2) mapping of the zenith delay with gradients (Brenot et al., 2014; Kačmařík and Rapant, 2012), in some cases separating the dry and wet part and using the appropriate mapping function (Champollion et al., 2009), or 3) mapping of the zenith delay with gradients and adding post-fit residuals (Bender et al., 2011b). Another aspect is the separation of the STD to Slant Hydrostatic Delay (SHD) and Slant Wet Delay (SWD). The GNSS processing cannot distinguish between the two parts and a combination of meteorological observations and empirical models is required to estimate the ZWD and the corresponding SWD (Bevis et al., 1994). This can either be done within the STD processing or as an independent step after the GNSS processing. Considerable errors can be introduced within the separation step as the SWD is only a small part of the STD (0-10 %) and small errors in the SHD can lead to severe errors in the SWD especially for dry periods. All of these approaches were used to process STDs for GNSS tomography experiments and realistic humidity fields could be obtained with any of the STD data sets. Even in direct comparison it is very difficult to identify the optimum strategy (Kačmařík et al., 2012).

Emerging new satellite systems and their signals might be used for strengthening the ZTD solutions and for improving the estimates of the atmospheric asymmetry in the vicinity of the GNSS receiver. Although the GLONASS system is still not officially operational, data are already collected and used. Since 2008, the IGS has provided ultra-rapid precise orbits for GLONASS satellites with contributions from at least 4 European ACs with products being sufficiently robust for generating operational multi-GNSS (GPS+GLONASS) NRT ZTD solutions (Douša, 2010). The initial inconsistency between standalone GPS and GLONASS ZTD solutions disappeared when the IGS08 antenna phase centre models were adopted (Dach et al., 2011b). Li et al. (2014b) reports on the first results of tropospheric monitoring with the Chinese BeiDou GNSS system. Initial problems still need to be resolved, namely enhanced processing software including strategies for optimal multi-signal and multi-frequency processing, support of precise orbit and clock products for the BeiDou satellites, and improved models for receiver and satellite phase antenna offsets and variations.

In 2010, the first operational global NRT ZTD estimates were provided by ACs at the UK Met Office and at GOP (Geodetic Observatory Pecny) with data from the GOP solution having been assimilated into the Met Office global NWP model since 2012 (Douša and Bennitt, 2013). Both systems apply the standard double-difference ZTD processing scheme. However, in the future the PPP technique can be applied in order to support an unlimited number of stations, with an almost homogeneous ZTD quality expected with some deviations due to regional quality variations in the global precise products.

The use of meteorological data as an input in GNSS processing has been limited. Climatological data were usually preferred for the utilization in GNSS analyses mainly for 1) developing mapping functions (which represent the tropospheric path delays at any elevation derived from the tropospheric delay at zenith above a GNSS receiver), and 2) separating hydrostatic and wet tropospheric components of the ZTD. In the last decade, the increasing demands of accuracy for positioning and navigation, increasing resolution of NWP models, and the direct use of actual meteorological data in space-based geodetic techniques has been explored. For example, the Vienna Mapping Function (VMF) concept provides a support for mapping functions derived from NWP models by applying the ray-tracing technique (Boehm and Schuh, 2004; Urquhart et al., 2013). The impact of the atmospheric loading effect based on actual meteorological data has also been evaluated by various ACs (e.g. Dach et al. (2011a)). Future services supporting GNSS with meteorological data as an input will further improve the temporal and spatial data resolution and will include modelling of atmospheric asymmetry (e.g. Boehm and Schuh (2007)). Other emerging fields for exploiting actual meteorological data are real-time precise positioning, navigation, and timing applications.

2.3 Reprocessed GNSS tropospheric products

Within EUREF (http://www.euref.eu), tropospheric parameter estimation started in 2001 as a Special Project. In 2008, the Special Project was declared successful and the troposphere product became a routine operation with daily delivery of a combined tropospheric solution. The EUREF Permanent Network (EPN, http://epncb.oma.be) is a key geodetic infrastructure coordinating a network of about 250 European GNSS stations. For each station, EUREF provides daily tropospheric estimates at 1-h sampling rate for the period 1996-present. More than 100 EPN stations are co-located with radiosondes, while only a small subset of stations are collocated with Very Long Baseline Interferometry (VLBI) radio telescopes. At these collocated sites, routine comparisons are carried out, which can be used for inter-technique evaluation (see Section 2.4). Taking benefit of more than 17 years of continuous GNSS observations in Europe, the second reprocessing activity (EPN-repro2) is ongoing using the latest available models and analysis strategy in order to provide an homogeneous GNSS time series suitable for monitoring climate. In 2007, a Memorandum of Understanding between EUREF and EUMETNET was signed to facilitate data exchange and to promote increasing cooperation between the geodetic and meteorological communities in Europe (Pottiaux et al., 2009).

Within IGS, global GNSS tropospheric products are produced operationally since 1997. Until 2003, the ZTD estimates consisted in a combined product derived from the contribution of the routinely produced ZTDs of several IGS analysis centres (Gendt, 1998). Due to large inconsistencies among analysis centres and changes over time in the estimation processes the legacy combination product was abandoned in 2003 to the profit of a new ZTD product derived from PPP processing by one centre (Byun and Bar-Sever, 2009). In 2008, IGS initiated the first reprocessing campaign (IGS-repro1, http://acc.igs.org) in order to provide a homogeneous time-series of the IGS core products and relevant derived products including tropospheric estimates. The reprocessing was done in three sequential steps: 1) nine ACs delivered global precise products, 2) those contributions were combined to produce the official IGS-repro1 orbit and clock products, and 3) homogeneous tropospheric parameters were calculated in 2010 using PPP for the period 1995 to 2007 (Bar-Sever, 2012). Using the same processing procedure, the IGS ZTD product was updated for the period 2007 to 2010 and continued operationally until mid 2011, giving hence access to a homogeneous ZTD series of more than 16 years. Since April 2011, the IGS tropospheric parameters are produced by United States Naval Observatory USNO, using PPP processing, but with a different software (Byram and Hackman, 2012). In 2013, a second IGS reprocessing campaign (IGS-repro2) was initiated from which a new reprocessed tropospheric product is expected.

In the last 5 years, reprocessing activities have been ongoing in many national agencies and GNSS ACs in Europe (regional and local reprocessing activities). It is to be noted that all reprocessing strategies require a well-documented, long-term metadata sets. Thus an effort will be required to archive the regional and national densification networks (data and metadata) for future reprocessing activities.

2.4 Inter-technique comparisons

Inter-comparisons are made for a number of reasons. When a new technique becomes available, as in the case of GNSS, it is naturally compared to existing techniques to assess its strengths and weaknesses. Atmospheric water vapour is difficult to measure with high accuracy, so when the GNSS technique appeared in the mid-nineties it was almost immediately also used as a reference, e.g., for evaluation of NWP models.

Weather balloons carrying radiosondes vertically up through the atmosphere are the classical meteorological in situ observation technique. In terms of its usage for direct comparison, the main disadvantages of radiosondes are that the measurement direction cannot be controlled (its horizontal path is determined by the wind speed and direction) and that it is not an instantaneous observation (the ascension of the balloon typically takes 1 to 2 hours). Both of these factors must be taken into account when radiosonde data is compared to other remote sensing observations.

Remote sensing of water vapour techniques may be divided into two categories: 1) differential time of arrival measurements, and 2) emission/absorption measurements. Differential time of arrival techniques were originally developed for positioning, navigation and timing applications with atmospheric water vapour content being a spin-off product from space-based geodetic data processing techniques. In addition to GNSS, there are two other techniques which use signals in the radio band of the electromagnetic spectrum, namely: Very Long Base Interferometry (VLBI) and Doppler Orbitography Radiopositioning Integrated by Satellite (DORIS).

Microwave radiometry from the ground measures the emission from atmospheric water vapour around the 22 GHz (MWR22) or the 180 GHz (MWR180) emission line. The 22 GHz system is the more common since it also works reasonably well in cloudy conditions, being able to correct for the influence of cloud water droplets on the total emission observed by using a second observation frequency. Both systems however do not provide any meaningful observation of atmospheric water vapour during rainy conditions. Additional ground-based techniques, which may observe in the visible band, comprise the CIMEL sun photometers from the AErosol RObotic NETwork (AERONET), and the Fourier Transform Infrared spectrometers (FTIR) observing solar absorption spectra.

The Advanced Microwave Sounding Unit-B (AMSU-B) is a satellite-based microwave instrument that can be used to infer the atmospheric water vapour content from several bands around the 180 GHz emission line from polar orbiting meteorological satellites. In the infrared and visible bands, satellite measurements are made with the Atmospheric Infrared Sounder (AIRS) and the GOME/SCIAMACHY/GOME-2 instruments, respectively.

Table 3 summarises a number of published studies that include the aforementioned instruments and techniques. These, together with references therein, provide extensive comparisons results. It is, however, not possible to draw final conclusions regarding the absolute accuracies of the instruments and techniques. All techniques suffer from systematic errors at different time scales meaning that case studies using specific sensors, at specific locations, at different times, will give different comparison results, often presented as biases and Root Mean Square (RMS) differences. For example an error appearing as a bias in a two-week long comparison may present itself as a random error over a period of many years.

It is not obvious that any of the techniques listed in Table 3 is superior in terms of accuracy: GNSS for example, suffers from systematic errors that depend on the elevation cut-off angle used in the processing scheme - by increasing elevation angle, the short-term (random) error increases but the stability over longer time periods is improved as systematic errors are more evident at low elevation angles (Ning and Elgered, 2012). The VLBI technique is not affected by multipath due to the large directivity of the radio telescopes. However, even though VLBI may be the most accurate technique available today, it has the large disadvantage in terms of acquiring operational data. VLBI measurements are only made at some tens of sites globally, the observations are not continuous, and each telescope can only measure in one direction at the time.

In conclusion, ground-based GNSS has short-term RMS errors around 3-4 mm in the ZTD, corresponding to 0.4-0.6 kg/m^2 in IWV. Systematic errors include: 1) satellite and receiver instrumentation effects (antenna phase center offsets and their variations, receiver code and phase delays), 2) in situ environmental effects (multipath, effects due to snow and ice on the antenna, monumentation), and 3) various modelling approximations such as mapping functions and methods for separation of the ZHD and the ZWD. For NRT applications and weather forecasting, systematic errors are less serious since it is the detection and timing of IWV changes that offers valuable information. For the extreme application of climate monitoring where stability over decades is required, GNSS is still a valuable technique, but here other space geodetic systems such as DORIS and, especially, VLBI can fulfil the role of maintaining the stability through collocated observations.

3 GNSS in NWP and weather forecasting

Comparison of GNSS tropospheric products to NWP model data, as well as use of the GNSS data in weather forecasting, has been investigated by many groups. Here we focus mainly on publications discussing this topic from a European perspective. The review is divided into subsections covering inter-comparison of GNSS and NWP model output (3.1.1), data assimilation (DA) and impact of GNSS data in NWP models (3.1.2), use of GNSS data by forecasters for nowcasting and severe weather monitoring (3.2), and finally GNSS water vapour tomography (3.3).

3.1 Usage of GNSS tropospheric products in NWP models

While much of the work of usage of GNSS data in weather forecasting is taking place at the National Meteorological Services (NMS), only some of these results are reported in refereed journals. In a few cases non reviewed and unpublished research is included in this review, in order to accurately present the current state-of-the-art regarding use of ground-based GNSS data in meteorology.

3.1.1 GNSS tropospheric products comparison with NWP

In Europe a multitude of NWP models are used by the NMS. For an overview of the configurations used, see the EUMETNET-SRNWP compilation at http://srnwp.met.hu. The majority of these models are developed in collaboration between NMSs in model consortia, see e.g. http://srnwp.met.hu/Consortia/ListofConsortia.html. A few additional, more freely available, NWP models are used at universities and other research institutions. Each NWP model has its own characteristics, resulting in parts of their behaviour being similar from institute to institute. However, NWP models are setup slightly differently, to suit local needs, and both the GNSS data processing and NWP models have been improved substantially during the time covered by this review.

For these reasons, biases between NWP and GNSS change with the model, but they also change with region (NMS) and with time. Similar for the changes in NWP model skill. Most of these variations are gradual, while a few are on/off in nature. For example, this regards the move to absolute antenna phase center calibration in GNSS data processing, which changed the GNSS bias relative to all NWP models; and it regards the use of observation operators and height corrections in NWP DA. The observation operators (calculating the GNSS equivalent, e.g. ZTD, from the NWP model variables) in different NWP models are not identical. In particular, they treat the ZTD contribution above the model top and the corrections for height offsets between GNSS antenna and model orography differently. These differences cause "artificial" systematic ZTD biases between NWP models, adding to the "real" biases resulting from slightly different humidity, pressure and temperature fields in the models. As long as the biases caused by the observation operator are not (or only weakly) weather dependent, they can effectively be negated by a bias correction prior to DA. However, this is something to be aware of when validating NWP against GNSS ZTD data. Use of GNSS data to validate the quality of NWP diurnal cycle variations in humidity is much less affected by the above mentioned bias changes. It should be noted that much of the work on comparisons cited below is from a time when the main issue was to document that GNSS ZTD estimates were useful to meteorology. A fundamental change took place in 2005, when E-GVAP was established to provide GNSS ZTDs specifically for operational meteorology, and the focus moved toward usage rather than validation.

Table 4 summarises comparisons of GNSS tropospheric products comparison with NWP models in Europe. Reported is: 1) pronounced seasonal cycle of GPS-NWP model bias and StDev (COSMO and HIRLAM), being largest in summer and smallest in winter, 2) bias and StDev decreased with altitude; bias almost constant with latitude, while StDev decreased with latitude (HIRLAM). In COSMO NWP model underestimation of IWV was found to correlate well with significant overestimation of light precipitation, suggesting coupling between the two components of the hydrological cycle. Reported is also systematic underestimation of the NWP model diurnal IWV cycle between 6 and 21 UTC (COSMO). The largest differences are observed at stations located in mountainous areas and/or near the sea, which reveal differences in model representativeness (ECMWF). Large GNSS-NWP model ZTD biases are found over limited periods of 1-3 days, mostly at coastal stations (ALADIN).

3.1.2 Assimilation of GPS tropospheric products in NWP models - impact studies and long term experiments

NWP is an initial value problem, the quality of the initial state is of crucial importance to the quality of the forecasts. The procedure of finding the initial state is called DA.

In most cases, such as in the most commonly used 3D-Var and 4D-Var (Var = variational) DA systems, the initial state is obtained by combining observations with an NWP field (a short-term forecast from the previous forecast cycle, the so-called first guess, valid at the time of the data analysis) before the start of the NWP forecast run. This is done in a statistical optimal way. The difference between 3D-Var and 4D-Var is that in the latter the time evolution within the DA time window, the period inside which the observations are selected, is taken into account, and that a time sequence of observations from a site can be used, while only one in 3D-Var. 4D-Var is mainly used for global models, with wide assimilation time windows, 6-12 hours, but in some cases also in regional models with more narrow assimilation windows.

Due to the inclusion of an error covariance matrix for the NWP model, and of physical balances in Var assimilation, a given observation will influence several model variables simultaneously, and in an extended region around the location of the observation. Each observation is associated with an observation error, including both the instrumental error and the so-called "error of representativeness". The latter is caused by the fact that the volume represented by the observation often differs from the resolution of the model. In most cases the observations are more local, i.e. for wind and temperature. Development of a Var-based assimilation system requires manpower and a powerful computer to run in an operational setting. It must be noted that different institutions using the same NWP model often use different approaches for ZTD bias correction as well as for selection of observations and determination of error statistics hence impact will vary from institution to institution

An alternative NWP DA technique is nudging. Instead of first making a separate data analysis, nudging is done by adding to the basic NWP model equations artificial forcing terms, the strength of which depends on the deviation between the NWP and the observations. For the part of the new forecast cycle for which fresh observations are available, one adds or nudges in the observations. When "now" is passed (no more new observations are available), the forecast becomes a truly free forecast. The benefit of nudging is it simplicity, the ease with which a whole time sequence of observations can be used, and the ability to use very recent observations. Some the drawbacks of the method are that one can only nudge in observations that correspond to model variables, or are somehow transformed to correspond to model variables, and less sophisticated quality control of observations. In practice nudging of GNSS data is done by first converting to IWV, then nudging humidity up or down in the column in the NWP model, depending on the NWP GNSS offset.

The impact of a new type of observations in NWP can be investigated in many ways. The most stringent is observing system experiments (OSE), in which two simulations are performed, one with and one without (the control run) assimilation of the new observations. It is important to observe which observations were used in the control runs. Often one will only consider the new observations in the development phase of a DA system, but for new observations to be of value in operational meteorology, they must add positive impact on top of all the other observations already being used, which is much more difficult to demonstrate. Objective verification of precipitation is notoriously difficult, mainly due to the lack of observation data with sufficient density in space and time in most countries. This is improving, mainly due to high-resolution observing techniques such as weather radars providing 2D precipitation data, but for the majority of the period covered in this review, subjective verification (comparison of precipitation maps to point observations) and point based verification have been the main tools.

Table 5 gives a summary of the DA techniques used to assimilate the GNSS tropospheric products. It can be seen that all NWP models used operationally in European have the capacity to assimilate ZTD, with the exception of the COSMO model, which is nudging based and uses IWV.

Most of the early studies, before 2005, showed a positive impact on short term precipitation forecasts from assimilation of GNSS data. Often most clearly seen by visual inspection of precipitation patterns, in particular regarding case studies of

Atmos. Meas. Tech. Discuss., doi:10.5194/amt-2016-125, 2016
Manuscript under review for journal Atmos. Meas. Tech.
Published: 6 June 2016

Atmospheric Measurement Techniques Discussions

heavy precipitation events. This is often associated with improvement in the humidity (compared to radiosonde and ground measurements) and of cloud cover. But sometimes negative effect were seen, e.g. a drying of the COSMO model winter time and increased over prediction of light rain (DMI HIRLAM), etc.

It is UK Met Office and Météo France that first started large scale operational use of GNSS data in Europe, following the establishment of E-GVAP in 2005. Today both institutions report a positive impact from use of GNSS data in both their regional and global NWP models. Several other institutions now use GNSS delay data operationally, but it is expected that many more will follow in the next few years.

Several institutions are now starting to run hourly rapid update cycle (RUC) models with hourly DA. Depending on the cut-off time, this requires faster access to GNSS ZTDs delivered from sub-hourly or RT GNSS processing systems. Such applications can be referred to as "NWP nowcasting". It does not differ greatly from standard NRT NWP, except the increased demand for higher resolution, high-frequency observations. In some cases the cut-off times are reduced so much that many "standard" observations have not arrived at the NMSes when the RUC DA is run, in which case they'll need to rely more heavily on specific frequent fast access observations, such as sub-hourly GNSS delays (de Haan, 2013).

3.1.3 Handling GNSS observation errors, variational bias control, observation error correlations and data thinning

The amount of ground based GNSS data is rapidly increasing, which calls for a higher degree of automatisation in estimation of observation errors and NWP versus GNSS biases. Schemes for variational bias control are being introduced and tested in both AROME (Moll et al., 2008) and HARMONIE (Arriola et al., 2016). Variational bias control enables usage of time varying biases in the DA, which is likely a benefit, since errors and biases are likely weather dependent. It is well established the O-B offsets have a seasonal dependence.

There is a huge range of NWP resolutions involved, grid box sizes running from about 60 km (ARPEGE on far side of the Earth seen from Paris) to 1.5 km in the latest UK Met Office local model. Many NMSes now run their high resolution models at about 2.5 km grid box size (AROME, COSMO, HARMONIE), many will move toward 1 km in the coming years. The NWP resolution is important for the optimal spatial density of the observations presented to the NWP DA system. Recently Météo France reduced their thinning distance to 10 km for AROME at 2.5 km grid box size, meaning effectively no data thinning at todays typical GNSS site inter distances. This increased the amount of sites used by a factor 4, and improved the forecasting skill of the AROME model at Météo France (Moll et al., 2008). More recently Szintai and Mile (2015) showed that for AROME over Hungary the effect of humidity observations per observation on the data analysis is larger than for other observations, and largest for GNSS ZTD, which indicates that the DA is system will benefit strongly from more of these observations. Indicating that we are far from saturation as regards the density of GNSS sites in the system. Similar indications have previously been found in case studies, where additional field campaign data were added to the operational GNSS ZTD data.

The quality of GNSS ZTD estimates systematically improve with time, from RT to NRT, and further on to post processed data. Within operational meteorology this is a highly uncommon issue, and meteorological databases and DA systems are not built to handle quality updates of the same property. In E-GVAP, this is currently handled by naming the solutions differently, e.g. METR vs. METO (sub- hourly vs. hourly). Handling this issue in a more systematic way, transparent to all users and data

Atmos. Meas. Tech. Discuss., doi:10.5194/amt-2016-125, 2016
Manuscript under review for journal Atmos. Meas. Tech.
Published: 6 June 2016

producers, will likely improve the impact of GNSS tropospheric products in NWP. The importance of this increases with the movement toward rapid update NWP with short cut-off times, while still running global NWP with 12 h DA time windows.

It is clear from the nature of GNSS processing, that GNSS ZTDs will have correlated errors in space and time. However, in NWP DA it is normally assumed that observations do not have correlated errors, which simplifies and speeds up the DA. If one assimilates observations with correlated errors, they will get a higher influence on the DA than they deserve according to their individual observations errors. While some work has been done to estimate the GNSS ZTD error correlations, very little work has been carried out to try to handle the correlations in the DA (see TOUGH Deliverables D19 and D22, http://tough.dmi.dk/deliverables/d19.html and http://tough.dmi.dk/deliverables/d22.html). A simpler hack is to reduce error correlations by data thinning, but as mentioned above indications are that more GNSS ZTDs are beneficial to the NWP DA.

3.1.4 Assimilation of STD and ZTD gradients

Assimilation of ZTD gradients and STD appears a natural next step in NWP usage of GNSS data.

In TOUGH, a 3D-Var assimilation operator for STD was implemented in HIRLAM (by R. Eresmaa, see TOUGH Deliverable D38, R. Eresmaa, http://tough.dmi.dk/deliverables/d38.html). Several NMSs worked on enabling slant estimation and a number of impact experiments were carried out. Some of this is documented in Eresmaa et al. (2007) and Jarvinen et al. (2007), who tested assimilation of both synthetic and real STD data. Synthetic data were found to result in reasonable analysis increments. However, the assimilation of real STDs was found to result in too large analysis increments. This could be reduced by reducing their weighting, to correct for error correlations between numerous slants from a single receiver. With the weights reduced, the impact on the analysis of specific humidity corresponds well to that of radiosonde in the same region. An earlier comparison of GNSS to NWP STDs was carried out by de Haan et al. (2002).

Zus et al. (2008) implemented a slant assimilation capability to the 4D-Var MM5 model and verified its functionality. The representation of model physics and horizontal diffusion in 4D-Var were found to be very important factors. In the assimilation experiments it was found that the assimilation improved O-B statistics and resulted in a reasonable impact on the analysis, which was confirmed by data from independent GNSS receivers and radiosondes. A comparison to weather radar data showed improved simulation of a convective system. Use of "simplified" physics in the 4D-Var MM5 model led to erroneous analyses.

Since COST-716 and TOUGH, the typical NWP resolution at operational NMSs has increased significantly. This is likely to benefit use of asymmetrical GNSS information, such as ZTD gradients and STD, in NWP DA schemes.

3.2 GNSS for monitoring severe weather events and operational nowcasting

Severe weather events are very diverse, from very cold winters to very hot summers, and the latest suggestion is that they are being observed more and more frequently (Field et al., 2012). One type of severe weather event is intense precipitation, often associated with strong convection, and potentially leading to flash floods, large economic losses, and the risk to life. Over the last years, several publications discussed the use of GNSS for studying the water vapour field, and the production of GNSS-based tailored products for severe weather event monitoring (Table 6).

Several authors studied the relationship between the water vapour field and the life cycle/intensity of precipitation systems. They found a clear relationship between the variations of the GNSS IWV, surface pressure, and precipitation intensity (e.g. in north of Spain during the period 2002-2010 (Seco et al., 2012)), a preference of frontal systems to develop where the largest amount of water vapour is available, and evidences that water vapour has a predominant role as a precursor for initiation of local convection (van Baelen et al., 2011). These convective systems are associated with typical water vapour configuration characteristics (such as a dry/wet contrast), rapidly changing over time. They can also be initiated due to the orography causing large transfer of water vapour amount e.g. between the plain and the mountains (Graham et al., 2012), visible in GNSS IWV, leading to convection and producing thunderstorms.

Various studies demonstrated the capability of GNSS to monitor small-scale water vapour structures associated with the initiation and development of convective systems: the link between the 2D moisture field (2D GNSS water vapour maps), the activity of the thunderstorm and the intense lightning is clearly established (de Haan, 2008) and can be used to identify situation of deep convection condition and provide nowcasting warnings (Brenot et al., 2013). The use of GNSS IWV to nowcast lightning activity was also investigated (Mazany et al., 2002). They demonstrated the capability of GNSS IWV combined with other meteorological parameters to provide a lightning prediction index, valid for the next couple of hours.

In their studies, these authors obtained clear evidences of the benefits that GNSS can bring to the monitoring of severe weather events. They also often mention that further research and developments are needed to improve and standardise their methods and to be able to use them in operational nowcasting. The availability of the ultra-fast/real-time GNSS-tailored products (Section 2.2) will undoubtedly boost this research field in a near future.

3.3 GNSS Tomography

The potential of dense GNSS networks for deriving spatially resolved humidity fields and the application of tomographic techniques was already emphasized by Ware et al. (2000) and Bevis et al. (1992). Bevis et al. (1992) suggested the setup of small and dense GNSS networks specifically designed for meteorological applications. Such networks have so far only been established for specific campaigns. However, nationwide geodetic GNSS networks are continuously expanding and the station density is in some regions sufficient for tomographic applications. Currently, there are active GNSS tomography groups in most European countries which develop and operate tomography systems (Brenot et al., 2014; Benevides et al., 2014; Reverdy et al., 2009; Champollion et al., 2009; Notarpietro et al., 2011; Miidla et al., 2008; Perler et al., 2011; Kačmařík and Rapant, 2012; Rohm, 2013; de Haan, 2008; Saqellari-Likoka and Karathanassi, 2008).

The basic idea of GNSS tomography is to combine a large number of signal delays, which cover most parts of the atmosphere from different directions in order to obtain a spatially resolved field of the atmospheric refractivity or humidity. A single STD is defined by

$$STD = 10^{-6} \int\limits_S N(s)\, ds + (S - G) \approx 10^{-6} \int\limits_S N(s)\, ds \qquad (5)$$

where the geometric delay $S - G = \int_s ds - \int_g ds$ describes the extra path length due to ray bending. This term is usually neglected in GNSS tomography. The refractivity N is related to the atmospheric quantities pressure, temperature and humidity

Atmos. Meas. Tech. Discuss., doi:10.5194/amt-2016-125, 2016
Manuscript under review for journal Atmos. Meas. Tech.
Published: 6 June 2016

Atmospheric Measurement Techniques Discussions

and $N(s)$ is the refractivity along the bended signal path. To obtain the 3D refractivity field a large number of STDs is required which are combined to the observation vector $\mathbf{m}$. The 3D refractivity field is mapped to the state vector $\mathbf{x}$ and the equations 5, which relate each single observation to the state $\mathbf{x}$, are combined to a vector operator $\mathbf{F}$. This leads to a non-linear vector equation

$$\mathbf{m} = \mathbf{F}(\mathbf{x}) \tag{6}$$

which needs to be solved for $\mathbf{x}$, i.e. the 3D refractivity field. The equation is non-linear as the bended signal paths depend on the unknown refractivity field. This leads to severe problems and a linearized form is derived where the signal paths are assumed to be known and to be independent from $\mathbf{x}$. The linearization does not necessarily require the signal paths S to be straight lines but this is usually assumed. To solve the equation numerically the problem is discretized and the 3D refractivity filed is defined on the nodes of a spatial grid. The linearized and discretized form of the integral in equations 5 leads to a weighted sum of the N_j along each signal path where the weights specify the contribution of each N_j to the signal delay i: $STD = m_i = \Sigma_j \omega_j N_j$. The weights ω_j can be combined to a matrix $\mathbf{A}$ which consists of one row i for each observation and one column j for each grid node and equation 6 can be written as a matrix vector product:

$$\mathbf{m} = \mathbf{A} \cdot \mathbf{x} \tag{7}$$

Only the weights ω_j, i.e. the matrix elements a_{ij}, near the signal path contribute to a given STD, all other matrix elements are filled with zeros. Consequently, the matrix $\mathbf{A}$ is a large sparse matrix. In general $\mathbf{A}$ is not a square matrix as the number of observations is not related to the number of grid nodes which define the refractivity field. The inverse matrix $\mathbf{A}^{-1}$ does therefore not exist and a least-squares solution does not provide a stable solution because $\mathbf{A}$ is a sparse ill-conditioned matrix.

This is typical for ill-posed problems which do in general not have a unique solution and the solutions are usually not stable. Regarding equations 7 there is in general an infinite number of different vectors x which would lead to the same set of observations $\mathbf{m}$ and small variations in the observations $\mathbf{m}$, e.g. observation errors, do lead to completely different solutions $\mathbf{x}$. Tomography leads in general to ill-posed problems and a large variety of solution strategies was developed. However, most of these strategies are not optimal for GNSS tomography. The GNSS ground networks used today were designed for geodetic applications with rather large inter-station distances and a inhomogeneous distribution of stations. The satellite-receiver links which "scan" the atmosphere vary with the satellite constellation and are highly variable in space and time. The properties of the operator $\mathbf{A}$ are therefore also time dependent which makes high demands on the inversion strategy.

The solution of equation 7 can be separated into 4 subtasks:

Discretisation The spatial discretisation of the atmospheric state defines the number of unknowns. A large number of N_j would be optimal to obtain a good approximation of equation 5 while a minimum number of unknowns would be best for the inversion of equation 7. The grid dimensions determine the number of STDs which are covered by the grid and the vertical distribution of nodes defines the vertical resolution, especially of the important boundary layer.

Atmos. Meas. Tech. Discuss., doi:10.5194/amt-2016-125, 2016
Manuscript under review for journal Atmos. Meas. Tech.
Published: 6 June 2016

Modelling of the operator A There is some freedom in the modelling of the operator $\mathbf{A}$, i.e. in the way to choose the weights $\omega_j = a_{ij}$ which relate the N_j to the integral $\int N ds$. In general a smooth operator with a small operator error would lead to more stable solutions.

Inversion strategy The choice of the inversion strategy depends on the properties of the operator $\mathbf{A}$. There is a large variety of standard techniques which can be used to solve equation 7.

Constraints The problem defined by equation 7 is globally underdetermined and additional observations or constraints are required to obtain stable solutions.

These four elements are essential for reliable and stable results but a continuously running tomography system is much more extensive.

The atmosphere is a dynamic system and observations made at different time are related to different atmospheric states. In an ideal case the tomography should use only STD observations from a certain time but the information provided by such a data set is usually insufficient to define the 3D refractivity field. The spatial information is therefore increased by collecting observations over longer periods, i. e. by reducing the temporal resolution. Depending on the sampling rate of the STD observations periods between 30 seconds (Perler et al., 2011) and 3 hours were used.

Some inversion algorithms require error estimates of the first-guess state and the observations as well. Depending on the data which enter the tomography efforts must be made to estimate the errors.

Another important factor is the processing of the STD observations which defines the observation error to a large degree. Many inversion algorithms show a tendency to amplify the observation errors which gives the STD processing strategy (see Section 2.2) a high impact on the performance of the entire tomography system. As it is not possible to separate the impact of the observation error from other influential factors this will not be further discussed in this section.

The GNSS tomography experiments reported so far are rather different in many respects and comparing the quality of the results is almost impossible. Furthermore, tomography results in large three dimensional fields but validation studies are usually limited to, e. g., a single radiosonde station or some horizontal layers and the relative performance of different approaches remains an open question. The current state of the European GNSS tomography will therefore be reviewed regarding the four criteria mentioned above. An overview about processing and inversion strategies can also be found in Notarpietro et al. (2011).

3.3.1 Spatial grid

The spatial discretization, i. e. the choice of a specific grid is an important issue and depends on the application. Large nationwide networks (Troller et al., 2006a; Bender et al., 2011a) require another grid than small limited area networks. In most experiments a regular horizontal grid is used, sometimes extended by a rather coarse outer grid around the region of interest (Troller et al., 2006a; Notarpietro et al., 2011). STDs at low elevations propagate through large parts of the atmosphere until the top layer of the grid is crossed, e. g. more than 50 km at an elevation of 10° and a height of 10 km. Extending grids around small networks is therefore a strategy to process STDs at low elevations, which provide most information about the vertical structure. It was found that the horizontal grid spacing should not be much smaller than the mean inter-station distance (Brenot

Atmos. Meas. Tech. Discuss., doi:10.5194/amt-2016-125, 2016
Manuscript under review for journal Atmos. Meas. Tech.
Published: 6 June 2016

et al., 2014; Bender et al., 2011a). The vertical grid spacing is usually chosen to increase with height thereby covering the important boundary layer with many cells but an equidistant spacing is also possible (Brenot et al., 2014; Bender et al., 2011a). The vertical resolution is limited to several hundred meters, ranging from 200-500 m near the ground, to 1-2 km at higher altitudes. It has been reported that the absolute location of the grid relative to the GNSS stations has a rather large impact on the results (Notarpietro et al., 2011; Chen and Liu, 2014).

3.3.2 Modeling of the operator

The discrete linear operator, i. e. the matrix $\mathbf{A}$, maps the state $\mathbf{x}$ on the observations $\mathbf{m}$ and the matrix elements a_{ij} specify the contribution of each grid node to a certain STD. One way for estimating the a_{ij} is provided by equation 5: The segments Δ_j in $\int N\,ds \approx \Sigma N_j\,\Delta_j$ can be regarded as the subpaths in each grid cell (= voxel) and N_j is the constant refractivity in each voxel. The latter assumption leads to a step function along the signal path and to rather large operator errors, especially for coarse grids. This approximation is used by almost all groups. However, discretization is not necessarily related to a voxel structure. The quantities at the grid nodes can always be interpolated on any point on the signal path providing a much smoother profile along the path. This leads to a much more realistic mapping from the grid to the STD and the error of the discretization is reduced (Perler et al., 2011). A non-linear operator which takes the ray bending into account could be developed using a ray-tracer (Zus et al., 2012).

3.3.3 Inversion strategy

Different inversion strategies are available to solve equation 7 and many of them were successfully applied to GNSS tomography.

The algebraic reconstruction techniques (ART) are a rather simple but fast iterative approach which applies small corrections to an initial state x_0 until a good approximation is obtained (Notarpietro et al., 2011; Bender et al., 2011b). There exists no general criterion when to stop the iteration, i. e. when the best approximation is found and oscillating or degrading situations need to be avoided. In most cases a good initial state is required to obtain stable results.

The pseudo inverse is an attempt to invert equation 7 which is based on the singular value decomposition (SVD) (Rohm, 2013; Flores et al., 2001). In case of ill-posed problems the SVD leads to a large number of very small singular values (large condition number of $\mathbf{A}$) which need to be truncated at an arbitrary level.

A weighted, damped least-squares solution of equation 7 can be found if an initial state is introduced (Reverdy et al., 2009; Baelen et al., 2011; Brenot et al., 2014; Benevides et al., 2014; Kačmařík and Rapant, 2012). This is equivalent to variational data assimilation where the difference to the observations and the initial state is minimized (de Haan, 2008). A more general approach is the Kalman filter which considers the errors of the initial state and the observations in a consistent way to provide the error of the final state (Perler et al., 2011; Rohm et al., 2014; Champollion et al., 2009; Miidla et al., 2008; Nilsson et al., 2007). The Kalman Filter seems to be the best established strategy but it leads to rather large matrices if a large number of observations needs to be processed or if the number of grid nodes becomes large. As the inverse of a large matrix needs to be computed this leads to rapidly growing processing times.

The inversion strategy might provide an optimal result but in case of globally underdetermined problems the optimum is very often a rather poor refractivity field with lots of artefacts. Up to now no superior inversion algorithm could be identified, good results were obtained with all of them but in case of insufficient observations all algorithms produce severe artefacts.

3.3.4 Constraints

Beyond the basic algorithms some constraints are required, as the problem is globally under-determined, and the solution is not unique anyway. The coverage of the atmosphere by slant paths is currently rather poor and many grid cells usually do not contain any observations. Therefore some extra information needs to be provided to obtain stable results, and to single out a meteorologicaly reasonable solution. This can be done in many different ways.

Inter-voxel constraints are used to distribute the STD information within the grid and to smooth strong gradients. They are usually realized as filters which replace the quantity at a specific node by a weighted sum over some neighboured region. Covariance functions with inverse distance weighting (Troller et al., 2006b) or Gaussian filters (Bender et al., 2011b) were implemented.

Boundary values help to keep the results within a meteorologicaly reasonable range and to reduce artefacts. The humidity above the tropopause is rather low and the top layer of the tomography grid between 8 and15 km can be set to zero humidity (Troller et al., 2006a). The surface layer (Bender et al., 2011b) or the all layers below a given height (Troller et al., 2006a) can be constrained by synoptic observations.

The STD distribution is very inhomogeneous which can lead to instable results full of artefacts. Pseudo observations are a way to obtain a more homogeneous STD distribution within all parts of the grid. Pseudo observations are built from real observations and some physical models and can be used to reduce the degree of ill-posedness of the inverse problem. As they do not add real information about the atmospheric state they usually have a strong smoothing effect.

The deficiencies of GNSS slant observations can be reduced by adding real observations from different sources: synoptic observations, radiosonde profiles, any kind of profiler data, radio occultation profiles or even GNSS ZWD/IWV data (Champollion et al., 2009). Extra data have usually a stabilizing effect on the inversion and act like constraints.

Most groups use combinations of constraints and additional observations to get stable and reliable results. Using a carefully tuned tomography system continuous series of stable results could be obtained which provide important information of the temporal development of the humidity filed (Brenot et al., 2014; Labbouz et al., 2013; Manning et al., 2012; Baelen et al., 2011)

3.3.5 Prospects of GNSS tomography

First GNSS tomography experiments were reported in the late 90th (Braun et al., 1999; Foelsche, 1999) describing the setup and results of rather small GPS networks. Today, after more than 15 years of experience, the networks were enlarged up to nationwide dimensions and numerous inversion strategies were tested but the GNSS tomography is still in an experimental state. There are two main reasons for the rather slow progress: 1) the number and density of observations is still insufficient compared with the dimensions of the atmosphere and the short correlation length of water vapor and 2) the inversion strategies investigated so far are not adequate to deal with the highly variable problem of GNSS tomography with an almost random distribution of GNSS stations and a fast changing satellite constellation. The degree of ill-posedness is changing with time and the inversion needs to address the variable character of the underlying mathematical problem. The standard techniques used so far are not optimal in this respect.

However, the future prospects of GNSS tomography are encouraging. Regarding the development of GNSS sites processed by E-GVAP within the last 10 years and the improvements in processing quality and speed it can be assumed that the density of GNSS stations and the quality of STD data becomes sufficient in a near future. Further improvements can be expected when GLONASS, BeiDou and Galileo tropospheric products become available. Advanced adaptive inversion techniques are currently developed and need to be applied to the GNSS tomography. Real-time humidity fields might in future be available on a national or even European scale, if efforts are made to densify the GNSS networks and to process STDs in a consistent way.

4 GNSS for climate monitoring

Atmospheric water vapour is the most abundant greenhouse gas involved in the climate feedback loop. As the temperature of the Earth's surface and atmosphere increases, so does the moisture-holding capacity of the atmosphere, and atmospheric water vapour is expected to increase in a warmer climate. Both climate models and observations indicate IWV increases by about 7 % per 1° C increase of temperature (Wentz and Schabel, 2000; Allen and Ingram, 2002; Trenberth et al., 2005; Held and Soden, 2006). Connected to such changes in the water vapour content are changes in the hydrological cycle, i.e. evaporation and precipitation (Bengtsson, 2010). The gradient in evaporation-precipitation increases proportionally to the lower tropospheric water vapour leading to larger differences between dry and wet areas. As a consequence, a good knowledge about the regional distribution of the water vapour content of the atmosphere is crucial as it ultimately determines the rate of precipitation.

Traditionally radiosondes and satellite observations have been used for IWV trend analyses. Gaffen et al. (1992); Ross and Elliott (1996, 2001) found an upward trend in the IWV from radiosonde measurements from 1973 to 1995 over North America, except for north-eastern part of Canada. They found increases over China and the Pacific Islands. Over the rest of Eurasia a mixture of positive and negative trends were found, with a tendency for negative trends over eastern Europe and western Russia. Trenberth et al. (2005) found that ocean satellite observations have a positive IWV trend of 0.40 kg/m^2 per decade from 1988 to 2003. However, despite a large radiosonde network the temporal resolution is low and differences in calibrations can give systematic errors in humidity (Wang and Zhang, 2008; Wang et al., 2013). Some remote sensing methods, observing in the infrared and the optical frequency bands, are limited to clear sky conditions. Other methods, using microwave remote sensing techniques, can be used also during cloudy conditions. On the other hand they only provide usable water vapour measurements over oceans (Trenberth et al., 2005). GNSS and DORIS can provide IWV observations with high accuracy that complement radiosonde and satellite measurements (Bock et al., 2007; Wang et al., 2007; Bock et al., 2010). As the time series of GNSS data grow longer they can also be used for the detection of trends and other systematic effects.

The capability of using GPS data to monitor climate changes (e.g. as a linear trends in IWV) has been investigated in a few studies only. The early attempts were made by Gradinarsky et al. (2002), who used data from 1993 to 2002 in Sweden, and

Atmos. Meas. Tech. Discuss., doi:10.5194/amt-2016-125, 2016
Manuscript under review for journal Atmos. Meas. Tech.
Published: 6 June 2016

Atmospheric Measurement Techniques Discussions
Open Access

found very small linear trends. In their study, the largest trend was seen at Onsala (0.2 kg/m^2 per year), on the Swedish west coast, where nearby microwave radiometer data and radiosonde data confirmed the GPS estimates. The study was completed by Nilsson and Elgered (2008); Jarlemark et al. (2010); Ning and Elgered (2012). These authors found IWV trends in the range from -0.5 kg/m^2 to +1.0 kg/m^2 per decade for the same area, but for different periods. They also studied several sources of uncertainty in the IWV trends due to natural variability of the IWV and errors in the GPS data (antenna phase centre variations, cut-off angle, multipath). Other studies provided IWV trend estimates and comparisons with independent data over specific regions (Morland et al., 2009; Sohn and Cho, 2010) or over the globe (Jin et al., 2009; Heise et al., 2009; Vey et al., 2010). Most notably, Vey et al. (2010) found good agreement between GPS estimates of seasonal and inter-annual variations in IWV and NCEP (National Center for Environmental Prediction) reanalysis, except in the tropics and in Antarctica, where the reanalysis underestimated IWV by 40 % and 25 %, respectively. Bock et al. (2014), also report IWV trends in the range $\pm$ 2 kg/m^2 per decade over the globe from GNSS and DORIS data which are in good agreement with ECMWF reanalysis (ERAInterim) and microwave satellite data (over the oceans). Vey et al. (2009) also investigated the homogeneity of the long-term GPS IWV series, and showed that offsets up to $\pm$ 1 kg/m^2 can arise, due to changes in antennas and radomes, and due to sudden changes in the number of observations, usually associated with failures in the equipment or changes in the observation cut-off angle. Changes in antenna phase centre or a varying environment affecting the signal multipath will affect the absolute level of the estimated IWV. Ning and Elgered (2012) showed that for some stations it can be an advantage to use elevation cut-off angles as high as 25°, in order to reduce such effects. The idea is that when searching for long-term trends, it can be acceptable that the uncertainty of individual estimates is increased if one at the same time reduces the size of systematic errors.

A recent comparison (Ning et al., 2013) with a regional climate model shows interesting systematic patterns (in both the phase and the amplitude) between coastal and inland sites, where the GNSS results in general confirm the variations seen in the climate model, although differences that call for more detailed studies also exist.

The application of GNSS for climate monitoring is an emerging new field of research. Ongoing reprocessing efforts within EUREF and IGS (see Section 2.3) using state-of-the-art models will provide a consistent time series of tropospheric data, taking benefit of 20 years of GNSS observations from over 400 stations worldwide and in Europe. One of the goals of the COST Action ES1206 (GNSS4SWEC) is to assess existing data sets of reprocessed GNSS ZTDs for the period from 1994 to present, standardise the ZTD to IWV conversion procedure and produce a homogenised data set. This unique data set will 1) enable validation and quantification of systematic biases from a range of instrumentation, 2) improve the knowledge of climatic trends, and 3) benefit both global and regional NWP reanalyses and climate model simulations through assimilation of GPS data or for validation purposes.

5 Conclusions

Application of GNSS for atmospheric sounding is now a well-established technique in Europe. Currently, the operational NRT tropospheric products, provided through E-GVAP, are used for validation and assimilation in a number of operational NWP models, used in reconstruction of 2D and 3D water vapour fields, and for impact studies of convection. However, there are yet further benefits to be obtained from innovation of the current operational GNSS tropospheric products. At present, most E-GVAP ACs process GPS-only data in a network solution providing hourly updated ZTD-only tropospheric products. Advanced GNSS tropospheric products such as horizontal ZTD gradients, STD (delays in the direction of each satellite), and 3D refractivity or humidity fields (using tomographic reconstruction) can now be produced.

Furthermore, multi-GNSS processing will improve the accuracy of tropospheric products due to increased number of observations and improved coverage of azimuth and elevation angles. Development and testing of new multi-GNSS products is of particular interest for operational NWP and forecasting of severe weather. Short-term, high-resolution NWP forecasting or nowcasting models require more detailed humidity observations than are currently available, especially to resolve small-scale phenomena like deep convection. Of particular interest in Europe are regional meteorological extremes such as heavy precipitation events, flash floods, and heat waves, which are expected to increase in the future as a result of global warming (Stocker et al., 2013). Relevant areas of research include: 1) severe weather forecasting: new GNSS products are required to provide additional information on the spatial heterogeneity and rapid temporal variability of tropospheric humidity, 2) nowcasting: providing rapid updates for the analysis of the atmospheric state requires a transition from NRT GNSS processing (as implemented in E-GVAP) to sub-hourly or real-time (PPP) processing schemes, and 3) multi-GNSS analysis combining data from GPS, GLONASS, Galileo and BeiDou are expected to provide improved estimates of tropospheric products.

The application of GNSS tropospheric products for climate monitoring is an emerging field of research. The use of GNSS estimates of the water vapour content in climate research has been limited so far, despite the good consistency in IWV trends derived from GNSS and other techniques (Ning and Elgered, 2012; Bock et al., 2014). Such results do however require homogeneous data sets. Over time, improvements in GNSS processing algorithms have introduced inconsistencies in long-term time series, making climate trend analysis challenging. Ongoing reprocessing efforts within the IGS and EUREF, using state-of-the-art GNSS processing, will provide a consistent time series of tropospheric data, taking benefit of nearly 20 years of GNSS observations from over 400 stations worldwide. These unique data sets will 1) enable validation and quantification of systematic biases from a range of instrumentation, 2) improve the knowledge of climatic trends of atmospheric water vapour, which currently have a large scatter, and 3) benefit both global and regional NWP reanalyses and climate model simulations (e.g. IPCC AR5).

More than 15 years of GNSS meteorology in Europe, has already achieved outstanding cooperation overcoming such difficulties as cross-border data access. Through collaboration between the atmospheric and geodetic communities in Europe it is now feasible to develop next-generation GNSS tropospheric products and applications that can enhance the quality of weather forecasts and climate monitoring. This work is carried out within the EU COST Action ES1206 "Advanced Global Navigation Satellite Systems tropospheric products for monitoring severe weather events and climate (GNSS4SWEC)" (2013-2017). GNSS4SWEC is targeting improved understanding of atmospheric processes that will result in more accurate nowcasting of severe weather. This will lead to improved hazard management, lowering the risk of loss of life and the risk to national infrastructure. GNSS4SWEC will also promote the use of re-processed long-term GNSS-based tropospheric delay data sets for climate research, with a focus on climate-sensitive regions such as higher latitudes. Correct representation of water vapour in climate models is essential for improvement of global warming and precipitation projections, on which the development of socio-economic response strategies are based. Also, the benefit to NWP and climate modelling in turn will lead to improved satellite-based positioning, navigation, and timing products through improved signal propagation models. In addition, while the production, exploitation, and evaluation of operational GNSS tropospheric products for NWP is a well-established research field in the northern and western Europe, it is still an emerging R&D field in eastern and south-eastern Europe. GNSS4SWEC is supporting the knowledge transfer and establishment of new ACs, which will benefit the operational E-GVAP service.

Author contributions. Guergana Guerova coordinated the writing of the manuscript and wrote sections 1 and 5 and contributed to section 3.1.1 and 3.1.2. Jan Douša, Galina Dick and Jonathan Jones wrote section 2.1 and section 2.2. Siebren de Haan contributed to section 3.1 and 3.2. Eric Pottiaux wrote section 3.2, contributed to section 2.1, section 2.2 and did final adjustments of the paper before submission. Olivier Bock contributed to section 4. Rosa Pacione wrote the EUREF reprocessing part of section 2.3 and contributed to section 4. Gunnar Elgered wrote section 2.4 and contributed to section 2.1 and 4. Henrik Vedel has major contribution to section 3.1 and wrote section 3.1.4 and 3.1.3. Michael Bender wrote section 3.3. All authors approved the entire manuscript before the final submission.

Data availability

The data for figure 2 is from E-GVAP service and is not publicly available yet.

Acknowledgements. The authors would like to acknowledge the support provided by COST - European Cooperation in Science and Technology for providing financial assistance for publication of the paper. Dr. W. Soehne, Federal Agency for Cartography and Geodesy (BKG), Germany, is acknowledged for the generation of the EUREF ZTD product. Dr. J. Douša acknowledges the national support from the Ministry of Education, Youth and Sports (LD14102). Dr. G. Guerova acknowledges supported through Marie Curie International Reintegration Grant (FP7-PEOPLE-2010-RG) of the 7th European Community Framework Programme. Dr. E. Pottiaux acknowledges the support of the Solar-Terrestrial Centre of Excellence (STCE), funded by the Belgian Federal Science Policy Office (BelSPO). Finally, the authors are grateful to the EUREF and the IGS, and all colleagues and data providers making GNSS meteorology and GNSS climate research possible.

References

Allen, M. R. and Ingram, W. J.: Constraints on future changes in climate and the hydrologic cycle, Nature, 419, 224–232, 2002.

Arriola, J. S., Lindskog, M., Thorsteinsson, S., and Bojarova, J.: Variational bias correction of GNSS ZTD in the HARMONIE modeling, J. Applied Metetorol., accepted, 2016.

Baelen, J. V., Reverdy, M., Tridon, F., Labbouz, L., Dick, G., Bender, M., and M.Hagen: On the relationship between water vapour field evolution and the life cycle of precipitation systems, Q. J. R. Meteorol. Soc., 137, 204–223, doi:10.1002/qj.785, http://onlinelibrary.wiley.com/doi/10.1002/qj.785/abstract, 2011.

Bar-Sever, Y.: IGSMAIL-6298, Reprocessed IGS Troposphere Product now available with Gradients, Email, http://igscb.jpl.nasa.gov/pipermail/igsmail/2010/007488.html., 2012.

Bauer, H.-S., Wulfmeyer, V., Schwitalla, T., Zus, F., and Grzeschik, M.: Operational assimilation of GPS slant path delay measurements into the MM5 4DVAR system, Tellus A, 63, 263–282, 2011.

Behrend, D., Haas, R., D. Pino, L. P. G., Keihm, S. J., Schwarz, W., Cucurull, L., and Rius, A.: MM5 derived ZWDs compared to observational results from VLBI, GPS and WVR, Phys. Chem. Earth, Part A, 27, 301–308, 2002.

Bender, M., Dick, G., Ge, M., Deng, Z., Wickert, J., Kahle, H.-G., Raabe, A., and Tetzlaff, G.: Development of a GNSS Water Vapor Tomography System Using Algebraic Reconstruction Techniques, Adv. Space Res., 47, 1704–1720, doi:10.1016/j.asr.2010.05.034, 2011a.

Bender, M., Stosius, R., Zus, F., Dick, G., Wickert, J., and Raabe, A.: GNSS water vapour tomography - Expected improvements by combining GPS, GLONASS and Galileo observations, Adv. Space Res., 47, 886–897, doi:10.1016/j.asr.2010.09.011, 2011b.

Benevides, P., Catalao, J., and Miranda, P. M.: Experimental GNSS tomography study in Lisbon (Portugal), Fisica de la Tierra, pp. 65–79, 2014.

Bengtsson, L.: The global atmospheric water cycle, Environ. Res. Lett., 5, 025 202, doi:10.1088/1748-9326/5/2/025202, 2010.

Bennitt, G. V. and Jupp, A.: Operational Assimilation of GPS Zenith Total Delay Observations into the Met Office Numerical Weather Prediction Models, Mon. Wea. Rev., 140, 2706–2719, doi:http://dx.doi.org/10.1175/MWR-D-11-00156.1, 2012.

Bevis, M., Businger, S., Herring, T. A., Rocken, C., Anthes, R. A., and Ware, R. H.: GPS Meteorology: Remote Sensing of Atmospheric Water Vapour Using the Global Positioning System, J. Geophys. Res., 97, 15 787–15 801, 1992.

Bevis, M., Businger, S., Chiswell, S., Herring, T. A., Anthes, R. A., Rocken, C., and Ware, R. H.: GPS Meteorology: Mapping Zenith Wet Delays onto Precipitable Water, J. App. Meteorol., 33, 379–386, doi:10.1175/1520-0450, 1994.

Bock, O., Keil, C., Richard, E., Flamant, C., and Bouin, M.-N.: Validation of precipitable water from ECMWF model analyses with GPS and radiosonde data during the MAP SOP, Q. J. R. Meteorol. Soc., 131, 3013–3036, doi:10.1256/qj.05.27, 2005.

Bock, O., Bouin, M. N., Walpersdorf, A., Lafore, J. P., Janicot, S., Guichard, F., and Agusti-Panareda, A.: Comparison of ground-based GPS precipitable water vapour to independent observations and NWP model reanalyses over Africa, Q. J. R. Meteorol. Soc., 133, 2011–2027, doi:10.1002/qj.185, 2007.

Bock, O., Willis, P., Lacarra, M., and Bosser, P.: An inter-comparison of zenith tropospheric delays derived from DORIS and GPS data, Adv. Space Res., 46, 1648–1660, doi:10.1016/j.asr.2010.05.018, 2010.

Bock, O., Willis, P., Wang, J., and Mears, C.: A high-quality, homogenized, global, long-term (1993-2008) DORIS precipitable water data set for climate monitoring and model verification, J. Geophys. Res., 119, 7209–7230, doi:10.1002/2013JD021124, 2014.

Boehm, J. and Schuh, S.: Vienna Mapping Function in VLBI Analysis, Geophys. Res. Let., 31, L01 603, doi:10.1029/2003GL018984, 2004.

Atmos. Meas. Tech. Discuss., doi:10.5194/amt-2016-125, 2016
Manuscript under review for journal Atmos. Meas. Tech.
Published: 6 June 2016

Boehm, J. and Schuh, S.: Troposheric gradients from the ECMWF in VLBI analysis, J. Geod., 81, 403–408, doi:10.1007/s00190-007-0144-2, 2007.

Braun, J., Rocken, C., Meertens, C., and Ware, R.: Development of a Water Vapor Tomography System Using Low Cost L1 GPS Receivers, in: Nineth ARM Science Team Meeting Proceedings, San Antonio, Texas, https://www.arm.gov/publications/proceedings/conf09/extended_abs/braun_j.pdf, braun J., C. Rocken, C. Meertens, and R. Ware. (1999), Development of a Water Vapor Tomography System Using Low Cost L1 GPS Receivers, Nineth ARM Science Team Meeting Proceedings, San Antonio, Texas, March 22-26., 1999.

Brenot, H., Ducrocq, V., Walpersdorf, A., Champollion, C., and Caumont, O.: GPS zenith delay sensitivity evaluated from high-resolution numerical weather prediction simulations of the 8-9 September 2002 flash flood over southeastern France, J. Geophys. Res., 111, D15 105, doi:10.1029/2004JD005726, 2006.

Brenot, H., Neméghaire, J., Delobbe, L., Clerbaux, N., De Meutter, P., Deckmyn, A., Delcloo, A., Frappez, L., and Van Roozendael, M.: Preliminary signs of the initiation of deep convection by GNSS, Atmos. Chem. Phys., 13, 5425–5449, doi:10.5194/acp-13-5425-2013, http://www.atmos-chem-phys.net/13/5425/2013/, 2013.

Brenot, H., Walpersdorf, A., Reverdy, M., van Baelen, J., Ducrocq, V., Champollion, C., Masson, F., Doerflinger, E., Collard, P., and Giroux, P.: A GPS network for tropospheric tomography in the framework of the Mediterranean hydrometeorological observatory Cévennes-Vivarais (southeastern France), Atmos. Meas. Tech., 7, 553–578, doi:10.5194/amt-7-553-2014, www.atmos-meas-tech.net/7/553/2014/ http://www.atmos-meas-tech.net/7/553/2014/amt-7-553-2014.html, 2014.

Buehler, S. A., Östman, S., Melsheimer, C., Holl, G., Eliasson, S., John, V. O., Blumenstock, T., Hase4, F., Elgered, G., Raffalski, U., Nasuno, T., Satoh, M., Milz, M., and Mendrok1, J.: A multi-instrument comparison of integrated water vapour measurements at a high latitude site, Atmos. Chem. Phys., 12, 10 925–10 943, doi:10.5194/acp-12-10925-2012, 2012.

Byram, S. and Hackman, C.: Computation of the IGS Final Troposphere Product by the USNO, IGS workshop poster presentation, 2012.

Byun, S. and Bar-Sever, Y.: A new type of troposphere zenith path delay product of the international GNSS service, J. Geod., 83, 367–373, doi 10.1007/s00190-008-0288-8, 2009.

Caissy, M., Agrotis, L., Weber, G., Hermandez-Pajares, M., and Hugentobler, U.: Innovation: Comming Soon: The International GNSS Real-Time Service, GPS World, 2012.

Champollion, C., Flamant, C., Bock, O., Masson, F., Turner, D., and Weckwerth, T.: Mesoscale GPS tomography applied to the 12 June 2002 convective initiation event of IHOP 2002, Q. J. R. Meteorol. Soc., 135, 645–662, doi:10.1002/qj.386, http://www3.interscience.wiley.com/journal/122274084/abstract, 2009.

Chen, B. and Liu, Z.: Voxel-optimized regional water vapor tomography and comparison with radiosonde and numerical weather model, J. Geod., doi:10.1007/s00190-014-0715-y, 2014.

Cucurull, L., Navascues, B., Ruffini, G., Elosegui, P., Rius, A., and Vila, J.: The use of GPS to validate NWP systems: the HIRLAM model., Journal of Atmospheric and Oceanic Technology, 17, 773–787, 2000.

Cucurull, L., van den Berghe, F., Barker, D., Vilaclara, E., and Rius, A.: Three-Dimensional Variational Data Assimilation of Ground-Based GPS ZTD and Meteorological Observations during the 14 December 2001 Storm Event over the Western Mediterranean Sea, Mon. Wea. Rev., 132, 749–763, doi:http://dx.doi.org/10.1175/1520-0493(2004)132<0749:TVDAOG>2.0.CO;2, 2004.

Dach, R., Boehm, J., Lutz, S., Steigenberger, P., and Beutler, G.: Evaluation of the impact of atmospheric pressure loading modeling on GNSS data analysis, J. Geod., 85, 75–91, doi:10.1007/s00190-010-0417-z, 2011a.

Dach, R., Schmid, R., Schmitz, M., Thaller, D., Schaer, S., Lutz, S., Steigenberger, P., Wuebbena, G., and Beutler, G.: Improved antenna phase center models for GLONASS, J. Geod., 15, 49–65, doi:10.1007/s10291-010-0169-5, 2011b.

Davis, J., Herring, T., Shapiro, I., Rogers, A., and Elgered, G.: Geodesy by radio interferometry: Effects of atmospheric modeling errors on estimates of baseline length, Radio science, 20, 1593–1607, 1985.

de Haan, S.: Meteorological applications of a surface network of Global Positioning System receivers, Ph.D. thesis, Wageningen Universiteit, http://www.knmi.nl/~haandes/, 2008.

de Haan, S.: Assimilation of GNSS ZTD and radar radial velocity for the benefit of very-short-range regional weather forecasts, Q. J. R. Meteorol. Soc., pp. 2097–2107, doi:10.1002/qj.2087, http://dx.doi.org/10.1002/qj.2087, 2013.

de Haan, S., van der Marel, H., and Barlag, S.: Comparison of GPS slant delay measurements to a numerical model: case study for a cold front passage, Phys. Chem. Earth., 27, 317–322, 2002.

Dick, G., Gendt, G., and Reigber, C.: First Experience with Near Real-Time Water Vapor Estimation in a German GPS Network, Journal of Atmospheric and Solar-Terrestrial Physics, 63, 1295–1304, 2001.

Douša, J.: Towards an Operational Near-real Time Precipitable Water Vapor Estimation, Phys. Chem. Earth, Part A, 26, 189–194, 2001a.

Douša, J.: The Impact of Ultra-Rapid Orbits on Precipitable Water Vapor Estimation using Ground GPS Network, Phys. Chem. Earth, Part A, 26, 393–398, 2001b.

Douša, J.: Precise near real-time GNSS analyses at Geodetic Observatory Pecny – precise orbit determination and water vapour monitoring, Acta Geodyn. Geomat., 7, 1–11, 2010.

Douša, J. and Bennitt, G. V.: Estimation and evaluation of hourly updated global GPS Zenith Total Delays over ten months, GPS Solutions, pp. 453–464, doi:10.1007/s10291-012-0291-7, 2013.

Douša, J. and Vaclavovic, P.: Real-time zenith tropospheric delays in support of numerical weather prediction applications, Adv. Space Res., 53, 1347–1358, doi:10.1016/j.asr.2014.02.021, 2014.

Dow, J. M., Neilan, R. E., and Rizos, C.: The International GNSS Service in a Changing Landscape of Global Navigation Satellite Systems, J. Geod., 83, 191–198, doi:10.1007/s00190-008-0300-3, 2009.

Elgered, G., Plag, H., Marel, H. V. D., Barlag, S., and Nash, J.: Action Number: 716 Exploitation of Ground-based GPS for Operational Numerical Weather Prediction and Climate Applications - Final Report, EU Publications Office (OPOCE), http://bookshop.europa.eu/uri?target=EUB:NOTICE:QSNA21639:EN:HTML, 2005.

Eresmaa, R., Järvinen, H., Niemela, S., and Salonen, K.: Azimuthal assummetry in ground-based GPS slant delay observations and their NWP model counterparst, Atmos. Chem. Phys. Discuss., 7, 3179–3202, 2007.

Eresmaa, R., Salonen, K., and Järvinen, H.: An observing-system experiment with ground-based GPS zenith total delay data using HIRLAM 3D-Var in the absence of satellite data, Q. J. R. Meteorol. Soc., 136, 1289–1300, doi:10.1002/qj.632, 2010.

Faccani, C., Ferretti, R., Pacione, R., Paolucci, T., Vespe, F., and Cucurull, L.: Impact of a high density GPS network on the operational forecast, Advances in Geosciences, 2, 73–79, doi:10.5194/adgeo-2-73-2005, http://www.adv-geosci.net/2/73/2005/, 2005.

Field, C., Barros, V., Stocker, T. F., Qin, D., Dokken, D. J., Ebi, K. L., Mastrandrea, M., Mach, K., Plattner, G., Allen, S., Tignor, M., and Midgley, P.: Managing the Risks of Extreme Events and Disasters to Advance Climate Change Adaptation. A Special Report of Working Groups I and II of the Intergovernmental Panel on Climate Change, Cambridge University Press, Cambridge, United Kingdom and New York, NY, USA, 2012.

Flores, A., Rius, A., de Arellano, J. V.-G., and Escudero, A.: Spatio-temporal tomography of the lower troposphere using GPS signals, Phys. Chem. Earth, Part A, 26, 405–411, 2001.

Foelsche, U.: Tropospheric water vapor imaging by combination of ground-based and spaceborn GNSS sounding data, Wissenschaftlicher Bericht No. 10, Karl-Franzens-Universität Graz, Institut für Meteorologie und Geophysik, 1999.

Gaffen, D. J., Elliott, W., and Robock, A.: Relationships between tropospheric water vapor and surface temperature as observed by radiosondes, Geophys. Res. Lett., 19, 1839–1842, 1992.

Gendt, G.: IGS combination of tropospheric estimates -The pilot experiment, 1997 technical reports, IGS, JPL, Pasadena, California, USA, edited by I. Mueller et al., 1998.

Gendt, G., Reigber, C., and Dick, G.: Near Real-Time Water Vapor Estimation in a German GPS Network - Results from the Ground Program of HGF GASP Project, Phys. Chem. Earth Part A, 26, 413–416, 2001.

Gendt, G., Dick, G., Reigber, C., Tomassini, M., Liu, Y., and Ramatschi, M.: Near real time GPS water vapor monitoring for numerical weather prediction in Germany, J. Meteor. Soc. Japan, 82, 361–370, doi:doi:10.2151/jmsj.2004.361, 2004.

Gradinarsky, L. P., Johansson, J., Bouma, H. R., Scherneck, H. G., and Elgered, G.: Climate monitoring using GPS, Phys. Chem. Earth, 27, 335–340, doi:10.1016/S1474-7065(02)00009-8, 2002.

Graham, E., Koffi, E. N., and Matzler, C.: An observational study of air and water vapour convergence over the western Alps during summer and the development of isolated thunderstorms, Meteorologische Zeitschrift, 21, 1–13, 2012.

Guerova, G. and Tomassini, M.: Monitoring IWV from GPS and limited - area forecast model, Tech. Rep. 2003-15, University of Bern, Switzerland, September 2003.

Guerova, G., Brockmann, E., Quiby, J., Schubiger, F., and Matzler, C.: Validation of NWP mesoscale models with Swiss GPS Network AGNES, Journal of Applied Meteorology, 42, 141–150, 2003.

Guerova, G., Bettems, J.-M., Brockmann, E., and Matzler, C.: Assimilation of the GPS-derived Integrated Water Vapour (IWV) in the MeteoSwiss Numerical Weather Prediction model - a first experiment, Phys. Chem. Earth., 29, 177–186, 2004.

Guerova, G., Brockmann, E., Schubiger, F., Morland, J., and Matzler, C.: An integrated assessment of measured and modeled IWV in Switzerland for the period 2001-2003, Journal of Applied Meteorology, 44, 1033–1044, 2005.

Guerova, G., Bettems, J.-M., Brockmann, E., and Matzler, C.: Assimilation of COST 716 Near Real Time GPS data in the nonhydrostatic limited area model used at MeteoSwiss, Meteorol. Atmos. Phys., 91, 149–164, doi:doi:10.1007/s00703-005-0110-6, 2006.

Haase, J., Calais, E., Talaya, J., Rius, A., Vespe, F., Santangelo, R., Huang, X.-Y., Davila, J. M., Ge, M., Cucurull, L., Flores, A., Sciarretta, C., Pacione, R., Boccolari, M., Pugnaghi, S., Vedel, H., Mogensen, K., Yang, X., and Garate, J.: The contributions of the MAGIC project to the COST 716 objectives of assessing the operational potential of ground-based GPS meteorology on an international scale, Physics and Chemistry of the Earth, Part A, 26, 433–437, 2001.

Haase, J., Ge, M., Vedel, H., and Calais, E.: Accuracy and Variability of GPS Tropospheric Delay Measurements of Water Vapor the Western Mediterranean, Journal of Applied Meteorology, 42, 1547–1568, 2003.

Heise, S., Dick, G., Gendt, G., Schmidt, T., and Wickert, J.: Integrated water vapor from IGS ground-based GPS observations: initial results from a global 5-min data set, Ann. Geophys., 27, 2851–2859, doi:10.5194/angeo-27-2851-2009, 2009.

Held, I. M. and Soden, B. J.: Robust responses of the hydrological cycle to global warming, J. Clim., 19, 5686–5699, 2006.

Henriksen, S. W., Mancini, A., and Chovitz, B. H., eds.: The Use of Artificial Satellites for Geodesy, American Geophysical Union, Washington, D. C., doi:10.1029/GM015p0247, 1972.

Jarlemark, P., Emardson, R., Johansson, J., and Elgered, G.: Ground-Based GPS for Validation of Climate Models: The Impact of Satellite Antenna Phase Center Variations, IEEE Geosci. Rem. Sens., 48, 3847–3854, doi:10.1109/TGRS.2010.2049114, 2010.

Jarvinen, H., Eresmaa, R., Vedel, H., Salonen, K., Niemela, S., and de Vries, J.: A variational data assimilation system for ground-based GPS slant delays, Q. J. R. Meteorol. Soc., 133, 969–980, 2007.

Jin, S. G., Luo, O. F., and Gleason, S.: Characterization of diurnal cycles in ZTD from a decade of global GPS observation, J. Geod., 83, 537–545, doi:10.1007/s00190-008-0264-3, 2009.

Johansson, J. M., Emardson, T. R., Jarlemark, P. O. J., Gradinarsky, L. P., and Elgered, G.: The atmospheric influence on the results from the Swedish GPS network, Phys. Chem. Earth, 23, 107–112, 1998.

Kačmařík, M. and Rapant, L.: New GNSS tomography of the atmosphere method – proposal and testing, in: Geoinformatics, edited by Čepek, A., vol. 9, pp. 63–76, Czech Technical University, Geoinformatics, http://geoinformatics.fsv.cvut.cz/pdf/geoinformatics-fce-ctu-2012-09.pdf, 2012.

Kačmařík, M., Douša, J., and Zapletal, J.: Comparison of GPS slant wet delays acquired by different techniques, Acta Geodynamica et Geomaterialia, 9, 427–433, 2012.

Keernik, H., Ohvrila, H., Jakobsona, E., Rannata, and Luhamaaa, A.: Column water vapour: an intertechnique comparison of estimation methods in Estonia, Proceedings of the Estonian Academy of Sciences, 63, 37–47, 2014.

Kehrer, K., Graf, B., and Roeder, W. P.: Global positioning system (GPS) precipitable water inforecasting lightning at spaceport Canaveral, Weather and Forecasting, 23, 219–232, 2008.

Kopken, C.: Validation of integrated water vapor from numerical models using ground-based GPS, SSM/I, and water vapor radiometer measurements, Journal of Applied Meteorology, 40, 1105–1117, 2001.

Labbouz, L., Baelen, J. V., Tridon, F., Reverdy, M., Hagen, M., Bender, M., Dick, G., and Gorgas, T.: Precipitation on the lee side of the Vosges Mountains: Multi-instrumental study of one case from the COPS campaign, Meteorologische Zeitschrift, 22, 413–432, doi:10.1127/0941-2948/2013/0413, http://www.schweizerbart.de, 2013.

Li, M., Li, W., Shi, C., Zhao, Q., Su, X., Qu, L., and Liu, Z.: Assessment of Precipitable Water Vapor Derived from Ground-based BeiDou Observations with Precise Point Positioning Approach, Adv. Space Res., doi:10.1016/j.asr.2014.10.010, 2014a.

Li, X., Dick, G., Ge, M., Heise, S., Wickert, J., and Bender, M.: Real-time GPS sensing of atmospheric water vapor: precise point positioning with orbit, clock and phase delay corrections, GeoResLet, 41, 3615–3621, doi:10.1002/2013GL058721, 2014b.

Mahfouf, J.-F., Boullut, N., Moll, P., Payan, C., Wattrelot, E., Augros, C., and Caumont, O.: Observation usage in Meteo France data assimilation systems: Current status and planned evolutions, Aladin workshop presentation, www.cnrm.meteo.fr/aladin/IMG/pdf/mahfouf.pdf, 2012.

Manning, T., Zhang, K., Rohm, W., Choy, S., and Hurter, F.: Detecting Severe Weather using GPS Tomography: An Australian Case Study, Journal of Global Positioning Systems, 11, 58–70, doi:10.5081/jgps.11.1.58, 2012.

Mazany, R., Businger, S., and Gutman, S.: A lightning prediction index that utilizes GPS integrated precipitable water vapor, Weather and forecasting, 17, 1034–1047, 2002.

Miidla, P., Rannat, K., and Uba, P.: Tomographys approach for tropospheric water vapour detection, CMAM, 8, 263–278, 2008.

Moll, P., Poli, P., and Ducrocq, V.: Use of ground based GNSS data in NWP at Météo-France, http://egvap.dmi.dk, e-GVAP expert team meeting, 2008.

Morland, J., Coen, M. C., Hocke, K., Jeannet, P., and Maetzler, C.: Tropospheric water vapour above Switzerland over the last 12 years, Atmos. Chem. Phys., 9, 5975–5988, doi:10.5194/acp-9-5975-2009, 2009.

Nilsson, T. and Elgered, G.: Long-term trends in the atmospheric water vapor content estimated from ground-based GPS data, J. Geophys. Res., 113, D19 101, doi:10. 1029/2008JD010110, 2008.

Nilsson, T., Gradinarsky, L., and Elgered, G.: Water vapour tomography using GPS phase observations: Results from the ESCOMPTE experiment, Tellus, 59A, 674–682, 2007.

Ning, T. and Elgered, G.: Trends in the atmospheric water vapor content from ground-based GPS: the impact of the elevation cutoff angle, IEEE Journal of Selected Topics in Applied Earth Observations and Remote Sensing, 5, 744–751, doi:10.1109/JSTARS.2012.2191392, 2012.

Ning, T., Haas, R., Elgered, G., and Willén, U.: Multi-technique comparisons of ten years of wet delay estimates on the west coast of Sweden, J. Geod., 86, 565–575, doi:10.1007/s00190-011-0527-2, 2012.

Ning, T., Elgered, G., Willen, U., and Johansson, J. M.: Evaluation of the atmospheric water vapor content in a regional climate model using ground-based GPS measurements, J. Geophys. Res., 118, 1–11, doi:10.1029/2012JD018053, 2013.

Notarpietro, R., Cucca, M., Gabella, M., Venuti, G., and Perona, G.: Tomographic reconstruction of Wet and Total Refractivity fields from GNSS receiver networks, Adv. Space Res., 47, 769–912, doi:10.1016/j.asr.2010.12.025, http://www.sciencedirect.com/science/journal/02731177/47/5, 2011.

Perler, D., Geiger, A., and Hurter, F.: 4D GPS water vapor tomography: new parameterized approaches, J. Geod., 85, 539–550, doi:10.1007/s00190-011-0454-2, 2011.

Poli, P., Moll, P., Rabier, F., Desroziers, G., Chapnik, B., Berre, L., Healy, S. B., Andersson, E., and Guelai, F.-Z. E.: Forecast impact studies of zenith total delay data from European near real-time GPS stations in Meteo France 4DVAR, J. Geophys. Res., 112, D06 114, doi:10.1029/2006JD007430, 2007.

Pottiaux, E., Bruyninx, C., Brockmann, E., and Söhne, W.: The EUREF-EUMETNET Collaboration: First experience and Potential Benefits, Bollettino di geodesia e scienze affini, 68, 269–286, 2009.

Reverdy, M., Baelen, J. V., Walpersdorf, A., Dick, G., Hagen, M., and Richard, E.: Water vapor fields retrieve with tomography software, Ann. Meteo., 44, 144–145, 2009.

Rohm, W.: The ground GNSS tomography – unconstrained approach, Adv. Space Res., 51, 501–513, doi:10.1016/j.asr.2012.09.021, http://www.sciencedirect.com/science/article/pii/S0273117712005935, 2013.

Rohm, W., Zhang, K., and Bosy, J.: Limited constraint, robust Kalman filtering for GNSS troposphere tomography, Atmos. Meas. Tech., 7, 1475–1486, doi:10.5194/amt-7-1475-2014, 2014.

Ross, R. J. and Elliott, W. P.: Tropospheric water vapor climatology and trends over North America: 1973–93, J. Climate, 9, 3561–3574, 1996.

Ross, R. J. and Elliott, W. P.: Radiosonde based northern hemisphere tropospheric water vapor trends, J. Climate, 14, 1602–1612, 2001.

Saqellari-Likoka, A. and Karathanassi, V.: An Approach for Solving Rank-Deficient Systems That Enable Atmospheric Path Delay and Water Vapor Content Estimation, IEEE Transactions on Geoscience and Remote Sensing, 46, 3187–3195, doi:10.1109/TGRS.2008.921744, 2008.

Schwitalla, T., Bauer, H.-S., Wulfmeyer, V., and Zängl, G.: Systematic errors of QPF in low-mountain regions as revealed by MM5 simulations., Meteorologische Zeitschrift, 17, 903–919, 2008.

Schwitalla, T., Bauer, H.-S., Wulfmeyer, V., and Aoshima, F.: High-resolution simulation over central Europe: assimilation experiments during COPS IOP 9c, Q. J. R. Meteorol. Soc., 137, 156–175, doi:10.1002/qj.721, 2011.

Seco, A., Ramirez, F., Serna, E., Prieto, E., Garcia, R., Moreno, A., Cantera, J. C., Miqueleiz, L., and Priego, J. E.: Rain pattern analysis and forecast model based on GPS estimated atmospheric water vapor content, Atmospheric Environment, 49, 85–93, 2012.

Sohn, D.-H. and Cho, J.: Trend Analysis of GPS Precipitable Water Vapor Above South Korea Over the Last 10 years, J. Astron. Space Sci., 27, 231–238, doi:10.5140/JASS.2010.27.3.231, 2010.

Spaenkuch, D., Gueldner, J., Steinhagen, H., and Bender, M.: Analysis of a dryline-like feature in northern Germany detected by ground-based microwave profiling, Meteorologische Zeitschrift, 20, 4, 409–421, 2011.

Steigenberger, P., Tesmer, V., Krügel, M., Thaller, D., Schmid, R., Vey, S., and Rothacher, M.: Comparisons of homogeneously reprocessed GPS and VLBI long time-series of troposphere zenith delays and gradients, J. Geod., 81, 503–514, doi:10.1007/s00190-006-0124-y, 2007.

Stocker, T. F., Qin, D., Plattner, G.-K., Tignor, M., Allen, S. K., Boschung, J., Nauels, A., Xia, Y., Bex, V., and Midgley, P. M., eds.: Climate Change 2013: The Physical Science Basis. Contribution of Working Group I to the Fifth Assessment Report of the Intergovernmental Panel on Climate change, Cambridge University Press, Cambridge, United Kingdom and New York, NY, USA, doi:10.1017/CBO9781107415324, 2013.

Suparta, W. and Ali, M.: Nowcasting the lightning activity in Peninsular Malaysia using the GPS PWV during the 2009 inter-monsoons, Annals of Geophysics, 57, A0217, 2014.

Szintai, S. and Mile, M.: Update of current status and plans of C-SRNWP, EUMETNET Obset expert team meeting, 2015.

Teke, K., Nilsson, T., Böhm, J., Hobiger, T., Steigenberger, P., Garcia-Espada, S., Haas, R., and Willis, P.: Troposphere delays from space geodetic techniques, water vapor radiometers, and numerical weather models over a series of continuous VLBI campaigns, J. Geod., 87(7), 981–1001, doi:10.1007/s00190-013-0662-z, 2013.

Tomassini, M., Gendt, G., Dick, G., Ramatschi, M., and Schraff, C.: Monitoring of integrated water vapor from ground-based GPS observations and their assimilation in a limited-area model, Phys. and Chem. of the Earth, 27, 341–346, 2002.

Tralli, D. M. and Lichten, S. M.: Stochastic estimation of tropospheric path delays in Global Positioning System geodetic measurements, Bulletin géodésique, 64, issue 2, 127–152, doi:10.1007/BF02520642, 1990.

Trenberth, K. E., Fasullo, J., and Smit, L.: Trends and variability in column-integrated atmospheric water vapor, Climate dynamics, 24, 741–758, 2005.

Troller, M., Geiger, A., Brockmann, E., Bettems, J.-M., Bürki, B., and Kahle, H.-G.: Tomographic determination of the spatial distribution of water vapor using GPS observations, Adv. Space Res., 37, 2211–2217, doi:10.1016/j.asr.2005.07.002, 2006a.

Troller, M., Geiger, A., Brockmann, E., and Kahle, H.-G.: Determination of the spatial and temporal variation of tropospheric water vapour using CGPS networks, Geophysical Journal International, 167, 509–520, 2006b.

Urquhart, L., Nievinski, F. G., and Santos, M. C.: Assessment of Tropospheric Mapping Functions Using Three-Dimensional Ray-tracing Through Numerical Weather Models., GPS Solutions, doi:10.1007/s10291-013-0334-8, 2013.

van Baelen, J., Reverdy, M., Tridon, F., L.Labbouz, Dick, G., Bender, M., and Hagen, M.: On the relationship between water vapour and evolution and the life cycle of precipitation systems, Q. J. R. Meteorol. Soc., 137, 204–223, 2011.

van der Marel, H., Brockmann, E., de Haan S, S., Douša, J., Johansson, J., Gendt, G., Kristiansen, O., Offiler, D., Pacione, R., Rius, A., and Vespe, F.: COST-716 demonstration project for the near real-time estimation of integrated water vapour from GPS, Phys. Chem. Earth, 29, 187–199, 2004.

van Malderen, R., Brenot, H., Pottiaux, E., Beirle, S., Hermans, C., Mazire, M. D., Wagner, T., Backer, H. D., and Bruyninx, C.: A multi-site intercomparison of integrated water vapour observations for climate change analysis, Atmos. Meas. Tech., 7, 2487–2512, doi:10.5194/amt-7-2487-2014, 2014.

Vedel, H. and Huang, X.-Y.: Impact of ground based GPS data on numerical weather prediction, J. Meteor. Soc. Japan, 82, 459–472, 2004.

Vedel, H., Mogensen, K. S., and Huang, X.-Y.: Calculation of zenith delays from meteorological data comparison of NWP model, radiosonde and GPS delays., Physics and Chemistry of the Earth, Part A: Solid Earth and Geodesy, 26, 497–502, 2001.

Vedel, H., Huang, X.-Y., Haase, J., Ge, M., and Calais, E.: Impact of GPS zenith tropospheric delay data on precipitation forecasts in Mediterranean France and Spain, Geophysical research letters, 31, 2004.

Vey, S., Dietrich, R., Fritsche, M., Ruelke, A., Steigenberger, P., and Rothacher, M.: On the homogeneity and interpretation of precipitable water time series derived from global GPS observations, J. Geophys. Res., 114, D10 101, doi:10.1029/2008JD010415, 2009.

Vey, S., Dietrich, R., Rlke, A., Fritsche, M., Steigenberger, P., and Rothacher, M.: Validation of precipitable water vapor within the NCEP/DOE reanalysis using global GPS observations from one decade, J. Climate, 23, 1675–1695, doi: 10.1175/2009JCLI2787.1, 2010.

Walpersdorf, A., Calais, E., Haase, J., Eymard, L., Desbois, M., and Vedel, H.: Atmospheric gradients estimated by GPS compared to a high resolution numerical weather prediction (NWP) model, Physics and Chemistry of the Earth, Part A, 26, 147–152, 2001.

Wang, J. and Zhang, L.: Systematic errors in global radiosonde precipitable water data from comparisons with ground-based GPS measurements, J. Climate, 21, 2218–2238, doi:10.1175/2007JCLI1944.1, 2008.

Wang, J., Zhang, L., Dai, A., van Hove, T., and van Baelen, J.: A near-global, 2-hourly data set of atmospheric precipitable water from ground-based GPS measurements, J. Geophys. Res., 112, D11 107, doi:10.1029/2006JD007529, 2007.

Wang, J., Zhang, L., Dai, A., Immler, F., Sommer, M., and Voemel, H.: Radiation dry bias correction of Vaisala RS92 humidity data and its impacts on historical Radiosonde data, J. Atmos. Oceanic Technol., 30, 197–214, doi:http://dx.doi.org/10.1175/JTECH-D-12-00113.1, 2013.

Ware, R. H., Fulker, D. W., Stein, S. A., Anderson, D. N., Avery, S. K., Droegemeier, R. D. C. K. K., Kuettner, J. P., Minster, J., and Sorooshian, S.: Real-time national GPS networks: Opportunities for atmospheric sensing, EPS, 52, 901–905, 2000.

Wentz, F. J. and Schabel, M.: Precise climate monitoring using complementary satellite data sets, Nature, 403, 414–416, 2000.

Yan, X., Ducrocq, V., Jaubert, G., Brousseau, P., Poli, P., Champollion, C., Flamant, C., and Boniface, K.: The benefit of GPS zenith delay assimilation to high-resolution quantitative precipitation forecasts: a case-study from COPS IOP 9, Q. J. R. Meteorol. Soc., 135, 1788–1800, doi:10.1002/qj.508, 2009a.

Yan, X., Ducrocq, V., Poli, P., Hakam, M., Jaubert, G., and Walpersdorf, A.: Impact of GPS zenith delay assimilation on convective-scale prediction of Mediterranean heavy rainfall, J. Geophys. Res., 114, D03 104, doi:10.1029/2008JD011036, 2009b.

Yang, H., Sass, B. H., Elgered, G., Johansson, J. M., and Emardson, T. R.: A comparison of precipitable water vapor estimates by an NWP simulation and GPS observations., Journal of Applied Meteorology, 38, 941–956, 1999.

Yuan, Y., Zhang, K., Rohm, W., Choy, S., Norman, R., and Wang, C. S.: Real-time retrieval of precipitable water vapor from GPS precise point positioning, J. Geophys. Res., 119, 10 044–10 057, doi:10.1002/2014JD021486, 2014.

Zumberge, J. F., Heflin, M. B., Jefferson, D. C., Watkins, M. M., and Webb, F. H.: Precise Point Positioning for the efficient and robust analysis of GPS data from large networks, J. Geophys. Res., 102/3, 5005–5017, 1997.

Zus, F., Grezeschik, M., Bauer, H.-S., Wulfmeyer, V., Dick, G., and Bender, M.: Development and optimisation of the IPM MM5 GPS slant path 4DVAR system, Meteorologische Zeitschrift, 17, 2008.

Zus, F., Bender, M., Deng, Z., Dick, G., Heise, S., Shang-Guan, M., and Wickert, J.: A methodology to compute GPS slant total delays in a numerical weather model, Radio Science, 47, RS2018, doi:10.1029/2011RS004853, http://www.agu.org/pubs/crossref/2012/2011RS004853.shtml, 2012.

Atmos. Meas. Tech. Discuss., doi:10.5194/amt-2016-125, 2016
Manuscript under review for journal Atmos. Meas. Tech.
Published: 6 June 2016

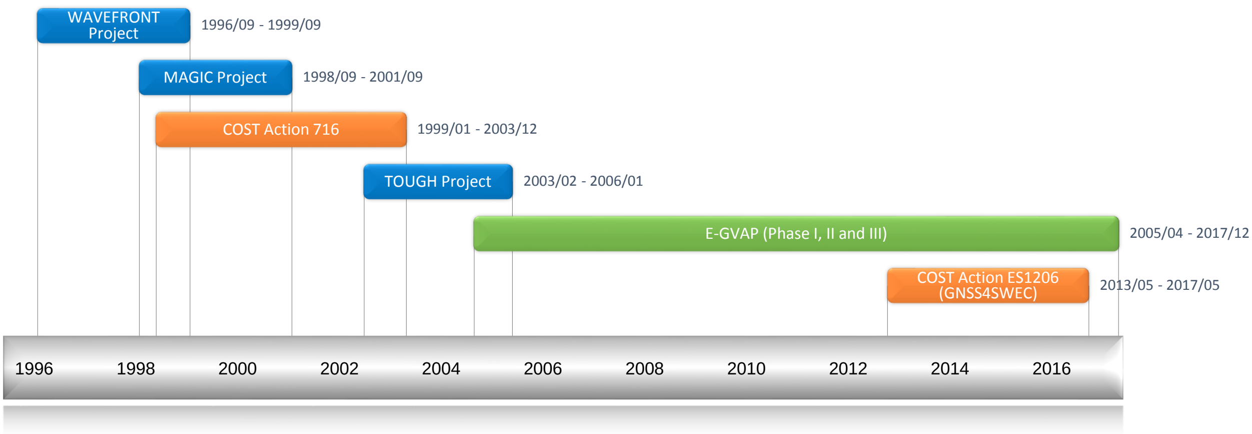

Figure 1. European GNSS Meteorology projects, from 1996 to present.

Table 1. Characteristics of the different GNSS tropospheric product type.

	Final Products	Near Real-Time (NRT) Products	Real-Time (RT) Products
GNSS data	Daily RINEX files	Hourly RINEX files	Real-time streams
GNSS products	Final	Ultra-rapid orbit (and clocks)	Real-time orbit (and clocks)
Models used in the analysis	Best available	Predicted or blind	Predicted or blind
Product availability	1 day - 2 weeks	90 min	5 - 10 min
Product in use since	after 1992	after 1999	after 2012

Table 2. PPP vs PNP GNSS processing strategy.

	Precise Point Positioning (PPP) (using raw observations)	Precise Network Positioning (PNP) (using double-differences)
Advantages	Small NEQ (clocks & ambiguities pre-eliminated)	Independence of external precise satellite clock products
	Station by station individual approach (keeping CPU with increasing number of sites/parameters (higher sampling rate, improved modeling etc.)	Sensitive to "relative" models and need "large" network
	Site dependent effects don't contaminate other solutions	Correlations between parameters of all stations taken into account
	Sensitive to absolute troposphere	
Disadvantages	Requires external precise satellite clock corrections consistent with orbits	Large normal equations
	Requires most precise models for undifferenced observations	Increasing CPU with increase number of sites/parameters
		Sensitive to "relative" model

Atmos. Meas. Tech. Discuss., doi:10.5194/amt-2016-125, 2016
Manuscript under review for journal Atmos. Meas. Tech.
Published: 6 June 2016

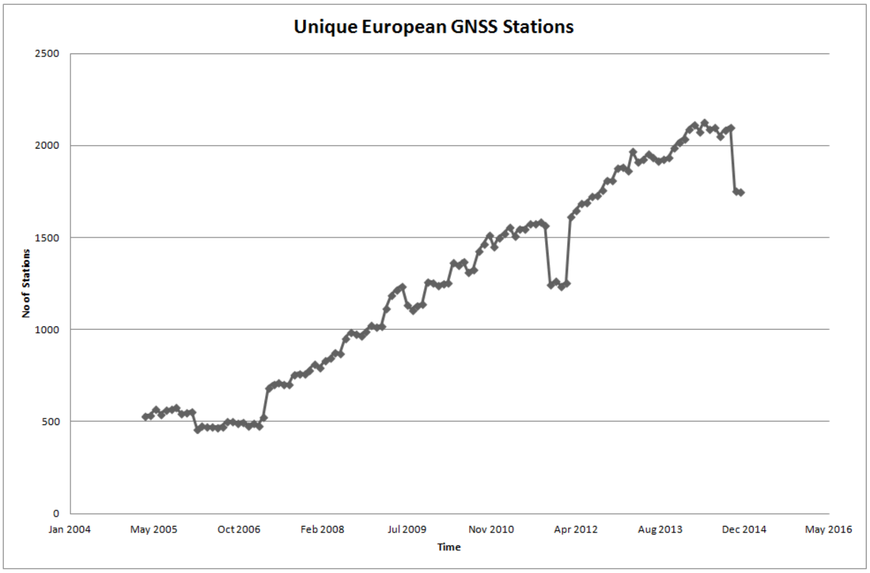

Figure 2. Number of ground-based GNSS stations delivering NRT ZTDs for operational NWP within E-GVAP.

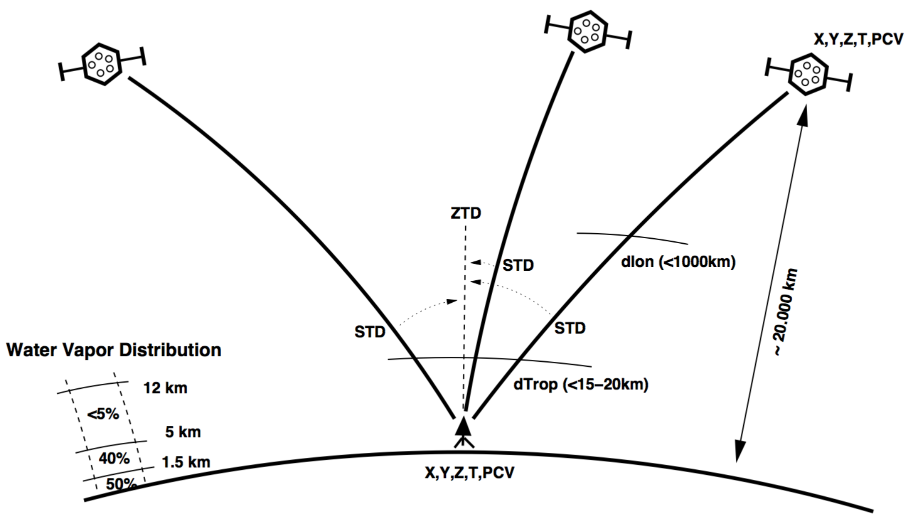

Figure 3. Schematic presentation of individual Slant Total Delays (STDs) from 3 GNSS satellites and their mapping to Zenith Total Delay (ZTD).

Atmos. Meas. Tech. Discuss., doi:10.5194/amt-2016-125, 2016
Manuscript under review for journal Atmos. Meas. Tech.
Published: 6 June 2016

Table 3. Selected comparisons of GNSS water vapour related studies.

Independent techniques*	Compared Parameters	Reference
VLBI	ZWD[1]	Steigenberger et al. (2007)
Radiosonde, VLBI, MWR22, NWM	ZWD[1]	Ning et al. (2012)
Radiosonde, AMSU-B, FTIR, MWR180, NWM	IWV[2]	Buehler et al. (2012)
VLBI, DORIS, MWR22, NWM	ZTD[3]	Teke et al. (2013)
DORIS, Radiosonde, NWM	ZTD[3], IWV[2]	Bock et al. (2014)
Radiosonde, AERONET, AIRS, GOME/SCIAMACHY/GOME-2	IWV[2]	van Malderen et al. (2014)

* The different techniques are further described in the text.

[1] Zenith Wet Delay, [2] Integrated amount of Water Vapour, [3] Zenith Total Delay

Table 4. Comparison of GNSS tropospheric products and NWP models in Europe.

NWP model*	Compared Parameters	Reference
HIRLAM	IWV[1]	Yang et al. (1999), Cucurull et al. (2000), Vedel et al. (2001), Haase et al. (2003), Keernik et al. (2014)
COSMO	IWV[1]	Kopken (2001), Tomassini et al. (2002), Gendt et al. (2004), Guerova and Tomassini (September 2003), Guerova et al. (2003, 2005)
ALADIN	IWV[1] ZTD[2]	Walpersdorf et al. (2001)
ECMWF	IWV[1]	Bock et al. (2005), Bock et al. (2007)
MM5	IWV[1]	Behrend et al. (2002), Schwitalla et al. (2008)

* The different models are further described in the text.

[1] Integrated amount of Water Vapour, [2] Zenith Total Delay

Atmos. Meas. Tech. Discuss., doi:10.5194/amt-2016-125, 2016
Manuscript under review for journal Atmos. Meas. Tech.
Published: 6 June 2016

Atmospheric Measurement Techniques Discussions
Open Access

Table 5. Assimilation of GNSS tropospheric products in NWP models.

NWP model	Assimilated Parameters	Method	Reference
HIRLAM	ZTD, STD	3D-Var 4D-Var	Vedel and Huang (2004), Vedel et al. (2004), Eresmaa et al. (2010), de Haan (2013)
COSMO	IWV, STD	Nudging Kalman filter	Tomassini et al. (2002), Gendt et al. (2004), Guerova et al. (2004, 2006)
ALADIN ALADIN+Meso-NH	ZTD	3D-Var	Brenot et al. (2006), Yan et al. (2009a), Mahfouf et al. (2012)
UK Metoffice *	ZTD	3D-Var 4D-Var	Bennitt and Jupp (2012), Douša and Bennitt (2013)
MM5	ZTD, IWV, STD	3D-Var 4D-Var Nudging	Cucurull et al. (2004), Faccani et al. (2005), Bauer et al. (2011)
AROME	ZTD	3D-Var	Moll et al. (2008), Yan et al. (2009b), Szintai and Mile (2015)
ARPEGE	ZTD	4D-Var	Poli et al. (2007)
HARMONIE	ZTD	3D-Var	Arriola et al. (2016)
WRF	ZTD	3D-Var 4D-Var	Schwitalla et al. (2011)

* The Met Office assimilates data in global and mesoscale model.

Table 6. Case studies of severe weather and operational nowcasting products.

Case study	Weather type	Reference
Mesoscale convective systems	intense precipitation	de Haan (2008), van Baelen et al. (2011), Graham et al. (2012), Brenot et al. (2013)
Thunderstorms	lightning	Mazany et al. (2002), Kehrer et al. (2008), Suparta and Ali (2014)
Warning Systems and 2D maps	all weather	de Haan (2008), Brenot et al. (2013)
Urban and rural IWV cycle		Champollion et al. (2009)
Synoptic scale	dry line, cyclones	Spaenkuch et al. (2011), Seco et al. (2012)